

IN THE UNITED STATES PATENT AND TRADEMARK OFFICE

Appl. No. : 10/563,211
Applicant : ULLRICH et al
Filed : January 4, 2006
TC/A.U. : 1643
Examiner : Sheela Jitendra Huff

Docket No. : 2923-743
Customer No. : 6449
Confirmation No. : 6030

Director of the United States Patent
and Trademark Office
P.O. Box 1450
Alexandria, Virginia 22313-1450

DECLARATION PURSUANT TO 37 C.F.R. § 1.132

I, Dr. Esther Zwick-Wallasch, declare as follows:

1. I have a Ph.D. in biology from the Max-Planck Institute for Biochemistry and relevant biological research experience as detailed in my *curriculum vitae*, which is attached. I consider myself to be at least as qualified as a person skilled in the field of pharmaceutical research and development.
2. I am familiar with U.S. Patent Application S.N. 10/563,211, which is directed to a method of preventing or treating an at least partially therapy-resistant hyperproliferative disorder comprising administering an inhibitor of a receptor tyrosine kinase ligand to a subject in need thereof, wherein said disorder is an at least partially irradiation- and/or medicament-resistant cancer.
3. I have read and am familiar with the currently outstanding Office Action issued in connection with this application by the U.S. Patent and Trademark Office on January 13, 2010. In that Action, the Examiner has reiterated the previous rejection of all of the claims under examination as allegedly lacking enablement for treating hyperproliferative cells *in vivo* by administering an inhibitor of a receptor tyrosine kinase ligand. The

Examiner has cited a number of references from the early to mid 1990's as evidence that there is not a predictable correlation between *in vitro* data and *in vivo* results.

4. The Examiner seems to be of the opinion that the *in vitro* data presented in the specification combined with the *in vivo* data from WO/2009/040134 do not show a correlation between *in vitro* and *in vivo* results. The Examiner is of the opinion that the *in vitro* assays in the WO 2009 reference need to be the same as used in the 10/563,211 application. The Examiner also contends that the *in vitro* assay used in the 10/563,211 application use siRNAs, while WO 2009 uses antibodies, and so there cannot be any correlation at all.

5. The 10/563,211 application discusses a number of receptor tyrosine kinase ligand inhibitors including antibodies or antibody fragments, proteinaceous or low-molecular weight inhibitors, and siRNAs (on pages 8 and 9 of the specification). The experimental data illustrated by Figures 3 and 4 and example result sections 2.3 and 2.4 relate to analysis of proHB-EGF release in response to stress agents and blockage of HB-EGF release by inhibitors. The data shows that stress agents induce phosphorylation of EGFR, and that inhibitors which inhibit HB-EGF or the release of tyrosine kinase ligands (EGF-like ligands) effectively block this phosphorylation (section 2.3 on pages 22-23 of the specification). The immunoblots show that inhibitors of HB-EGF (CRM197) and those which inhibit the release of EGF-like ligands (BB94) inhibit EGFR activation (Figure 3) and that it was shown that these inhibitors block HB-EGF release (Figure 4). An anti-HB-EGF antibody is used in the HB-EGF release assay demonstrating its binding to proHB-EGF (Figure 4a).

6. It is my expert opinion that a correlation between the *in vitro* data in this application and the *in vivo* results in the WO 2009 exists. The *in vitro* data in the present application shows that EGFR activation and release of HB-EGF is blocked by a specific inhibitor of HB-EGF (CRM197) and by a metalloprotease inhibitor, which inhibit the release of HB-EGF and other EGF-like ligands, in several human tumor cell lines and that anti-HB-EGF antibodies do indeed bind to proHB-EGF. There is disclosure in WO

2009 that “[w]hether an amino acid change results in a functional antibody, i.e., in an antibody that binds to HB-EGF and reduces, neutralizes or substantially inhibits the function of HB-EGF, can readily be determined by assaying the specific activity of the resulting antibody in ELISA or FACS for binding to HB-EGF or *in vitro* or *in vivo* functional assay,” (paragraph [000207]). Further, the *in vitro* data in WO 2009 that shows that anti-HB-EGF antibodies inhibit EGFR phosphorylation in human tumor cells (see paragraphs [000302-000305] and Figure 22, 23 and 24), as well as *in vivo* data showing that anti-HB-EGF antibodies cause reduced pancreatic tumor (Fig. 37) and ovarian cancer tumor growth (Fig. 38A-C) in mice. Data in WO 2009 demonstrates that the HB-EGF inhibitor CRM197, which is used in the 10/563,211 application as well as anti-HB-EGF antibodies block EGFR activation in Cos-7 cells stimulated by the G-protein-coupled receptor ligand LPA (Figure 23), which leads to extracellular processing of transmembrane growth factor precursor and release of mature growth factor, which interacts with the ectodomain of the EGFR and activates it through tyrosine phosphorylation (Prenzel et al., 1999, Nature 402:884-888). Thus, because this application shows binding of anti-HB-EGF antibodies to HB-EGF (Figure 4a) and that inhibitors of HB-EGF and those which inhibit the release of HB-EGF and EGF-like ligands block the release of HB-EGF in Cos-7 cells (Figure 4) and inhibit activation and phosphorylation of EGFR in Cos-7, TCC-Sup and NCI-H292 cells, (Figure 3) and WO 2009 shows that an inhibitors of HB-EGF, namely anti-HB-EGF antibodies bind to HB-EGF and inhibit activation and phosphorylation of EGFR in LPA-stimulated Cos-7 cells and also shows that this same inhibitor reduces tumor growth in mice, there is clearly a correlation between the *in vitro* results presented in this application and the *in vitro* and *in vivo* results shown in WO 2009.

7. With regard to the Examiner's contention that WO 2009 does not show an *in vivo* data using siRNAs and that gene therapy is not enabled, I am enclosing a paper entitled “Intravenous RNA Interference Gene Therapy Targeting the Human Epidermal Growth Factor Receptor Prolongs Survival in Intracranial Brain Cancer” by Zhang et al, which provides an excellent demonstration of the correlation of *in vitro* assays with *in vivo*

efficacy with regard to the use of EGFR inhibitors, specifically siRNAs, for treatment of cancer.

8. Zhang et al. detail *in vitro* and *in vivo* experiments, wherein, in cultured glioma cells, the delivery of the RNAi expression plasmid resulted in a 95% suppression of EGFR function, and weekly i.v. RNAi gene therapy caused reduced tumor expression of immunoreactive EGFR and an 88% increase in survival time of mice with advanced intracranial brain cancer (abstract). The first paragraph of the discussion section on page 3673 states that “[t]he results of these studies are consistent with the following conclusions. First, it is possible to knock down *EGFR* gene expression with i.v. gene therapy that uses expression plasmids encoding a shRNA directed at nucleotides 2529–2557 of the human EGFR mRNA (Table 2).” This shows the *in vitro* effects of an inhibitor of a receptor tyrosine kinase ligand in cells. Further, this data demonstrates successful gene therapy *in vitro*. Further, “EGFR expression knockdown is demonstrated by the inhibition of thymidine incorporation or calcium flux in human U87 glioma cells in tissue culture (Tables 2 and 3; Fig. 3), by the decrease in the expression of immunoreactive EGFR in cell culture (Fig. 2).” Thus, the *in vitro* effect of an inhibitor of a receptor tyrosine kinase ligand is demonstrated **in tissue**. Correlation of the *in vitro* results with *in vivo* effectiveness is also provided in the same paragraph based on the disclosure that there is a “decrease in brain cancer expression of immunoreactive EGFR *in vivo* (Fig. 6). Third, anti-EGFR gene therapy has an antiangiogenic effect and results in a 72–80% decrease in vascular density of the tumor (Fig. 5; Table 4).” With regard to gene therapy *in vivo*, the same paragraph states that “weekly i.v. anti-EGFR gene therapy results in an 88% increase in survival time in adult mice with intracranial brain cancer (Fig. 4).”

9. Thus, it is my expert opinion that, at the time of filing of the present invention, one of skill in the art would have recognized that there was a reasonable correlation between the *in vitro* results shown in the present application with *in vivo* utility in treating tumors because it was known that “EGFR plays an oncogenic role in 70% of solid cancers that originate outside the brain (2)” (page 3667 of Zhang et al. citing Nicholson et al., Eur. J.

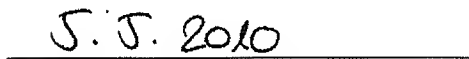
Cancer, 2001) and that knocking down its expression, e.g., by gene therapy, would be a way to treat cancer. See, e.g., Zhang et al., page 3667. It is also my expert opinion that a correlation between the *in vitro* use and *in vivo* utility of siRNAs was established. Therefore, the 10/563,211 application shows the *in vitro* use of siRNAs for gene therapy to inhibit endogenous expression of ADAM proteases to regulate EGFR activation in Cos-7 cells and lung cancer cells, and Zhang et al. shows the *in vitro* use of siRNAs for gene therapy to knock down EGFR expression in glioma cells and increase survival of mice *in vivo*. Thus, one of ordinary skill would have been enabled in treating a therapy-resistant hyperproliferative disorder by administering an inhibitor of a receptor tyrosine kinase ligand to a subject in need thereof.

10. I further declare that all statements made herein of my own knowledge are true and that all statements made on information and belief are believed to be true; and further that these statements were made with the knowledge that willful false statements and the like so made are punishable by fine or imprisonment, or both, under Section 1001 of Title 18 of the United States Code, and that such willful false statements may jeopardize the validity of the application or any patent issued thereon.

Dr. Esther Zwick-Wallasch



(signature)



Date

Enclosures: Zhang et al., Clinical Cancer Research, 2004, *curriculum vitae*.

CURRICULUM VITAE

Esther Zwick-Wallasch

Business Address U3 Pharma GmbH
Fraunhofertstr. 22, 82131 Gauting
E-mail: zwick-wallasch@u3pharma.com

Private Address Frühlingstr. 112, 82131 Gauting

Education

2000 **PhD in Biology**, Max-Planck Institute for Biochemistry,
Department Molecular Biology, Martinsried, Germany,
Supervisor: Prof. Dr. A. Ullrich

1995 **Diploma in Biology** (M.Sc. equivalent), Julius-Maximilians
University Würzburg, Supervisor: Prof. Dr. F. Grummt
Major in Biochemistry, Minors in Developmental Biology and
Immunology

1990-1994 **Study of Biology**, Julius-Maximilians University Würzburg

1990 **Abitur**, Trifels-Gymnasium Annweiler a. Trifels

Professional Experience

2008 – today **Director R&D**, U3 Pharma, Daiichi Sankyo
As global project leader responsible for pre-clinical
development of a monoclonal antibody project targeting an
EGF ligand.

2007 **Maternity leave**

2006 – 2007 **Program director**, U3 Pharma
As project leader responsible for in vitro pharmacology of a
humanized antibody project targeting an ion channel.

2001 – 2006 **Scientist**, U3 Pharma
As project leader responsible for the establishment of a cell-
based tyrosine kinase transactivation assay for the
implementation of a high-throughput screen (HTS) to identify
small molecule inhibitors.

2001 **Co-founder of U3 Pharma**

2000 – 2001 **Post-doctoral Fellow**, Max-Planck-Institute for Biochemistry,
Dept. Molecular Biology, Prof. Dr. A. Ullrich.
Working on transactivation of epidermal growth factor (EGF)
receptor via G-protein coupled receptors in cancer cells.

1995 – 2000 **Graduate Student**, Max-Planck-Institute for Biochemistry,
Dept. Molecular Biology, Prof. Dr. A. Ullrich.
PhD thesis on the mechanism of G-protein coupled receptor-
induced epidermal growth factor (EGF) receptor signal
transactivation pathway in neuronal cells.

1994 – 1995 **Undergraduate Student**, Max-Planck-Institute for
Biochemistry, Dept. Molecular Biology, Prof. Dr. A. Ullrich.
Diploma thesis on tissue-specific expression of protein-tyrosine
phosphatases in early embryonic development of mice.

Awards

2001

MPIB Junior Research Award of the Max-Planck-Institute of Biochemistry for outstanding research in cell biology and biochemistry.

2000

Otto-Hahn-Medal of the Max-Planck-Institute for the research into the mechanism of EGF receptor signal transactivation in neuronal cells.

Publications

Gómez-Varela D, **Zwick-Wallasch E**, Knötgen H, Sánchez A, Hettmann T, Ossipov D, Weseloh R, Contreras-Jurado C, Rothe M, Stühmer W, Pardo LA.
Monoclonal antibody blockade of the human Eag1 potassium channel function exerts antitumor activity.
Cancer Res. 2007 Aug 1;67(15):7343-9.

Hart S, Fischer OM, Prenzel N, **Zwick-Wallasch E**, Schneider M, Hennighausen L, Ullrich A.
GPCR-induced migration of breast carcinoma cells depends on both EGFR signal transactivation and EGFR-independent pathways.
Biol Chem. 2005 Sep;386(9):845-55.

Zwick E, Bange J, Ullrich A.
Receptor tyrosine kinases as targets for anticancer drugs.
Trends Mol Med. 2002 Jan;8(1):17-23. Review.

Zwick E, Bange J, Ullrich A.
Receptor tyrosine kinase signalling as a target for cancer intervention strategies.
Endocr Relat Cancer. 2001 Sep;8(3):161-73. Review.

Bange J, **Zwick E**, Ullrich A.
Molecular targets for breast cancer therapy and prevention.
Nat Med. 2001 May;7(5):548-52. Review.

Gschwind A, **Zwick E**, Prenzel N, Leserer M, Ullrich A.
Cell communication networks: epidermal growth factor receptor transactivation as the paradigm for interreceptor signal transmission.
Oncogene. 2001 Mar 26;20(13):1594-600. Review.

Prenzel N, **Zwick E**, Leserer M, Ullrich A.
Tyrosine kinase signalling in breast cancer. Epidermal growth factor receptor: convergence point for signal integration and diversification.
Breast Cancer Res. 2000;2(3):184-90. Epub 2000 Mar 25. Review.

Zwick E, Wallasch C, Ullrich A.
HER2/neu: a target for breast cancer therapy.
Breast Dis. 2000;11:7-18.

Prenzel N, **Zwick E**, Daub H, Leserer M, Abraham R, Wallasch C, Ullrich A.
EGF receptor transactivation by G-protein-coupled receptors requires metalloproteinase cleavage of proHB-EGF.
Nature. 1999 Dec 23-30;402(6764):884-8.

Zwick E, Hackel PO, Prenzel N, Ullrich A.
The EGF receptor as central transducer of heterologous signalling systems.
Trends Pharmacol Sci. 1999 Oct;20(10):408-12. Review.

Zwick E, Wallasch C, Daub H, Ullrich A.
Distinct calcium-dependent pathways of epidermal growth factor receptor transactivation and PYK2 tyrosine phosphorylation in PC12 cells.
J Biol Chem. 1999 Jul 23;274(30):20989-96.

Hackel PO, **Zwick E**, Prenzel N, Ullrich A.
Epidermal growth factor receptors: critical mediators of multiple receptor pathways.
Curr Opin Cell Biol. 1999 Apr;11(2):184-9. Review.

Zwick E, Daub H, Aoki N, Yamaguchi-Aoki Y, Tinhofer I, Maly K, Ullrich A.
Critical role of calcium- dependent epidermal growth factor receptor transactivation in PC12 cell membrane depolarization and bradykinin signaling.
J Biol Chem. 1997 Oct 3;272(40):24767-70.

Kharitonov A, Schnekenburger J, Chen Z, Knyazev P, Ali S, **Zwick E**, White M, Ullrich A.
Adapter function of protein-tyrosine phosphatase 1D in insulin receptor/insulin receptor substrate-1 interaction.
J Biol Chem. 1995 Dec 8;270(49):29189-93.

Humanized Gene Replacement in Mice Reveals the Contribution of Cancer Stroma-Derived HB-EGF to Tumor Growth

Tomoko Ichise¹, Satoshi Adachi¹, Minako Ohishi¹, Masahito Ikawa², Masaru Okabe², Ryo Iwamoto¹, and Eisuke Mekada^{1*}

¹Department of Cell Biology, Research Institute for Microbial Diseases, Osaka University, Osaka 565-0871, Japan, ²Department of Experimental Genome Research, Research Institute for Microbial Diseases, Osaka University, Osaka 565-0871, Japan

ABSTRACT. Tumor progression is a complex process that involves the interaction of cancer cells with the cancer-surrounding stromal cells. The cancer stroma influences the cancer cell growth and metastatic potential. The EGF family growth factor HB-EGF is synthesized in cancer cells and plays pivotal roles in oncogenic transformation and tumor progression, but the contribution of HB-EGF expressed in tumor stromal cells to tumor growth remains unclear. In the present study, we found that HB-EGF was expressed in host-derived cancer stromal cells in xenograft and allograft mouse tumor models. CRM197 is a specific inhibitor of human HB-EGF that has no effect on mouse HB-EGF. To elucidate whether host-derived stromal HB-EGF contributes to tumor growth, we generated knock-in mice expressing a CRM197-inhibitable humanized mutant form of HB-EGF. Administration of CRM197 to humanized knock-in mice that were bearing tumors derived from human or mouse cancer cells revealed that inhibition of host-derived stromal HB-EGF by CRM197 significantly reduced tumor growth. These results suggest that HB-EGF in the cancer-associated stroma plays a significant role for tumor growth, and that the HB-EGF derived from the stroma, as well as that expressed by cancer cells, is a potential target for cancer therapy. The present results also suggest that the humanized HB-EGF knock-in mice could be utilized for pathophysiological studies of HB-EGF as well as the development of therapeutic strategies targeting HB-EGF.

Key words: HB-EGF/CRM197/diphtheria toxin/stroma/tumorigenesis

Introduction

Tumor progression is a complex process that involves the interaction of cancer cells with the cells in the cancer-surrounding tissues (cancer stroma) including endothelial cells, fibroblasts, lymphocytes, and other cell types. The cancer stroma directly or indirectly influences cancer cell growth and metastatic potential (Bhowmick *et al.*, 2004; Folkman and Shing, 1992; Kalluri and Zeisberg, 2006; Mueller and Fusenig, 2004; Tlsty and Coussens, 2006). Although much attention has recently been paid to the roles

of the cancer stroma in tumor development and progression, the molecular mechanism underlying the crosstalk between cancer cells and stromal cells remains largely unknown.

The ErbB family of receptor tyrosine kinases and their ligands, the epidermal growth factor (EGF) family, play important roles in tumorigenesis (Normanno *et al.*, 2003). Heparin-binding EGF-like growth factor (HB-EGF), a member of the EGF family, is synthesized as a membrane-anchored form (proHB-EGF) and its soluble form is subsequently released from the cell surface by ectodomain shedding (Goishi *et al.*, 1995; Higashiyama *et al.*, 1991). The soluble HB-EGF has potent mitogenic and chemoattractant activities for a number of cell types (Higashiyama *et al.*, 1993). Increasing evidence has accumulated to indicate that HB-EGF plays pivotal roles in oncogenic transformation, tumor invasion and metastasis (Bos *et al.*, 2009; Miyamoto *et al.*, 2004; Miyamoto *et al.*, 2006; Ongusaha *et al.*, 2004), and that HB-EGF elaborated by cancer cells themselves is involved in tumorigenesis. However, the con-

*To whom correspondence should be addressed: Eisuke Mekada, Department of Cell Biology, Research Institute for Microbial Diseases, Osaka University, 3-1 Yamadaoka, Suita, Osaka 565-0871, Japan.

Tel: +81-6-6879-8286, Fax: +81-6-6879-8289

E-mail: emekada@biken.osaka-u.ac.jp

Abbreviations: EGF, epidermal growth factor; HB-EGF, heparin-binding EGF-like growth factor; proHB-EGF, membrane-anchored form of HB-EGF; DT, diphtheria toxin; hHB-EGF, human HB-EGF; mHB-EGF, mouse HB-EGF; hzHB-EGF, humanized HB-EGF; tRA, all-*trans* retinoic acid.

tribution of HB-EGF expressed in tumor stromal cells to tumor growth remains unclear, although HB-EGF is often expressed in fibroblasts and endothelial cells (Raab and Klagsbrun, 1997).

ProHB-EGF serves as the receptor for diphtheria toxin (DT) (Iwamoto *et al.*, 1994). DT and CRM197, a non-toxic mutant form of DT, bind to the EGF-like domain of human HB-EGF (hHB-EGF), thereby inhibiting the binding of hHB-EGF to EGF receptor (Mitamura *et al.*, 1995). Consequently, CRM197 is used as a specific inhibitor of hHB-EGF. Furthermore, it strongly inhibits tumor growth in mouse xenograft tumor models (Miyamoto *et al.*, 2004). However, CRM197 does not bind to mouse HB-EGF (mHB-EGF) and cannot inhibit mHB-EGF derived from cancer stromal cells in mouse tumor models (Mitamura *et al.*, 1995). In the present study, we generated knock-in mice in which the mHB-EGF gene was replaced with CRM197-inhibitable humanized HB-EGF (hzHB-EGF) and studied the role of HB-EGF produced by cancer stromal cells in tumor growth.

Materials and Methods

Reagents

DT and CRM197 were prepared as described previously (Uchida *et al.*, 1973).

Cell culture

All cell lines were maintained in DMEM supplemented with 100 U/ml penicillin G, 100 µg/ml streptomycin and 10% fetal bovine serum (ICN Biomedicals, Costa Mesa, CA, USA).

Plasmid construction and transfection

The constructions of plasmids encoding hHB-EGF cDNA, mHB-EGF cDNA and human/mouse HB-EGF chimeras inserted into the eukaryotic expression vector pRc/CMV (Invitrogen, Tokyo, Japan) were described previously (Mitamura *et al.*, 1995). For the construction of hzHB-EGF, we used the H (106–186) chimera HB-EGF cDNA as the starting material for hzHB-EGF construction (Mitamura *et al.*, 1995). This cDNA encodes mouse HB-EGF containing human sequence between Asp¹⁰⁶ and Tyr¹⁸⁶. The EGF-like domain locates between Cys¹⁰⁸ and Pro¹⁴⁹. Two amino acid residues in the sequence from Pro¹⁴⁹ to Tyr¹⁸⁶ differ between human and mouse HB-EGF. In order to restrict the substitution within the EGF-like domain, R153P and I162V mutations were introduced into the H (106–186) chimera HB-EGF cDNA inserted into the pRc/CMV vector by site-directed mutagenesis, resulting in an hzHB-EGF cDNA. A *Hind*III-*Msc*I fragment of the hzHB-EGF cDNA inserted into the pRc/CMV vector was substituted with the corresponding fragment of the H (54–73) chimera HB-EGF cDNA inserted into the pRc/CMV vector, resulting in an H6-hzHB-EGF

cDNA. Stable transfectants of LC cells expressing H6-mHB-EGF, hHB-EGF, H6-hzHB-EGF or hzHB-EGF were obtained by transfection with the corresponding plasmids using Lipofectamine 2000 (Invitrogen, Tokyo, Japan) according to the manufacturer's instructions.

DT sensitivity assay and DT binding assay

DT sensitivity was measured by inhibition of protein synthesis by DT as described previously (Umata *et al.*, 1990). Binding of DT to cells was measured as described previously (Iwamoto *et al.*, 1994).

Mitogenic assay

L cells (5×10^5 cells) were transfected with hHB-EGF, hzHB-EGF, H6 epitope-tagged hzHB-EGF (H6-hzHB-EGF) or H6 epitope-tagged mHB-EGF (H6-mHB-EGF) and cultured in RPMI 1640 containing 10% fetal calf serum and 10 µg/ml of heparin for 72 h. The conditioned media were collected. The mitogenic activities of HB-EGF in the conditioned media with and without CRM197 were assayed by measuring their effects on the proliferation of DER cells as described previously (Takazaki *et al.*, 2004).

Animal experiments

All experimental use of animals complied with the Guidelines for Animal Care of Osaka University.

Generation of humanized HB-EGF knock-in mice

A 6.0-kb *Eco*RI-*Sac*II fragment containing exon 1 of the HB-EGF gene and an 8.0-kb *Eco*RI-*Eco*RV fragment downstream of exon 3 were used as homology arms. A LoxP-flanked mHB-EGF cDNA with a poly(A) signal, a neo cassette driven by the phosphoglycerate kinase promoter and intron 5 of the mHB-EGF gene as a splicing donor (SD) were fused at exon 1. The hzHB-EGF cDNA linked to the GFP cDNA with a poly(A) signal via the internal ribosome entry site (IRES) was inserted downstream of intron 5 of the mHB-EGF gene (SD). The *Xho*I-linearized DNA of the targeting vector was electroporated into D3 embryonic stem (ES) cells. To obtain the HB^{hz-flox} allele, individual clones were screened for homologous recombination by Southern blot analysis of *Hind*III-digested DNA and *Spe*I-digested DNA with 5' and 3' probes that corresponded to sequences flanking the targeting vector of the 5'- and 3'-arms, respectively. *Spe*I-digested DNA was also analyzed with a neo probe as an internal probe. Hybridization was carried out as described previously (Iwamoto *et al.*, 2003).

The targeted ES clones were injected into C57BL/6J blastocysts, and the chimeric mice were bred with C57BL/6J female mice to obtain HB^{hz-flox} mice. Homozygous HB^{hz-flox/hz-flox} mice were obtained by interbreeding of HB^{hz-flox} mice. Subsequently, homozygous HB^{hz-flox/hz-flox} mice were bred with CAG-Cre transgenic mice (Sakai and Miyazaki, 1997) to generate HB^{hz/+} mice. Cre-mediated recombination was confirmed by PCR analysis using primer sets for Cre (fwd, 5'-AGGTTTCGTTCACTCATGGA-3' and rev, 5'-

TCGACCAGTTTAGTTACCC-3'), neo (fwd, 5'-ATGGGATCGGCCATTGAACA-3' and rev, 5'-GAAGAACTCGTCAAGAA-GGC-3') and GFP (fwd, 5'-CAAGCAGATCCTGAAGAACA-3' and rev, 5'-GAACATCTCCTCGATCAGGT-3') as well as a wild-type allele-specific primer set (wt) (fwd, 5'-CATGGGGTTGTG-ACTCTCCT-3' and rev, 5'-AGCCTGCACACACAAAAGTG-3'). Finally, HB^{h/z} heterozygous mice were intercrossed to generate HB^{h/z/h/z} mice. Elimination of mouse HB-EGF and alternative expressions of hzHB-EGF and GFP were confirmed by RT-PCR analysis using an hHB-EGF-specific primer set (fwd, 5'-ATGT-GAAGGAGCTCCGGG-3' and rev, 5'-TCAGTGGGAGCTAGC-CAC-3'), an mHB-EGF-specific primer set (fwd, 5'-ACCTGCAG-GAGTTCCGTA-3' and rev, 5'-TCAGTGGGAGCTAGCCAC-3'), a primer set based on the consensus sequence of hHB-EGF and mHB-EGF (fwd, 5'-ATGAAGCTGCTGCCGTCCGT-3' and rev, 5'-TCAGTGGGAGCTAGCCACGC-3'), a primer set for GFP and a primer set for G3PDH (fwd, 5'-ACCACAGTCCATGCCAT-CAC-3' and rev, 5'-TCCACCACCCTGTTGCTGTA-3').

RT-PCR

cDNAs were prepared by a reverse transcriptase, ReverTra Dash (Toyobo, Osaka, Japan) from total RNA extracted using ISOGEN (Nippon Gene, Tokyo, Japan) from all-*trans* retinoic acid (tRA)-treated mouse skins, and PCR was performed by using the primer sets as described above. (Yamazaki *et al.*, 2003).

Immunohistochemistry

HB^{del/+};nu/nu mice were obtained by crossing HB^{del/+} mice with nude (nu/nu) mice. A total volume of 0.1 ml containing 5×10^6 cells suspended in serum-free DMEM was subcutaneously injected into the HB^{del/+};nu/nu mice at 5 weeks of age. At 4 weeks after the tumor cell injection, the formed tumors were excised, fixed with 4% paraformaldehyde and embedded in OCT compound (Sakura Fine-Tek, Tokyo, Japan). Frozen sections (8 mm) were stained with 5-bromo-4-chloro-3-indolyl β -D-galactoside (X-Gal) and an anti-CD31 antibody (clone MEC13.3; BD PharMingen, Franklin Lakes, NJ, USA) or anti- α -smooth muscle actin (SMA) antibody (clone 1A4; Sigma, Tokyo, Japan). Other mouse tissues, including the hearts, were fixed by perfusion of 4% paraformaldehyde, dehydrated and embedded in paraffin. Paraffin sections (4 mm) were stained with hematoxylin/eosin or subjected to Azan-Mallory staining.

Effect of CRM197 on tumor growth in nude mice

A total volume of 0.1 ml containing 5×10^6 cells suspended in serum-free DMEM was subcutaneously injected into nu/nu mice or HB^{h/z/h/z}; nu/nu mice at 5 weeks of age. At several time points after the cell injection, the sizes of the tumors were measured using a caliper. The tumor volumes were calculated as described previously (Bissery *et al.*, 1991). CRM197 was dissolved in 1 ml of PBS containing 8% sucrose at 2.88 mg/ml and then further diluted to 8 μ g/ml with saline. CRM197 at a dose of 0.2 mg/kg was injected intraperitoneally into the tumor-bearing mice every day.

Statistics

The statistical significance was determined by Student's *t* test as implemented by Excel 2007 (Microsoft Corp., Redmond, WA, USA).

Results and Discussions

Cancer-associated stromal cells express HB-EGF

Cancer stroma expresses a number of growth factors, cytokines and chemokines to enhance cancer cell proliferation and metastasis. However, the expression of HB-EGF in cancer stroma has not yet been reported. We examined whether HB-EGF was expressed in cancer-associated stromal cells upon tumor formation. To this end, we utilized an HB-EGF^{del/+} lacZ reporter allele (Iwamoto *et al.*, 2003). In HB-EGF^{del/+} mice, lacZ is expressed under the HB-EGF promoter and localized in the nucleus because of an additional nuclear localizing signal, thereby enabling us to detect HB-EGF expression by lacZ staining. To facilitate the implantation of cancer cells into mice, HB^{del/+};nu/nu mice were used for this study. Tumors were generated by subcutaneously injecting human or mouse cancer cell lines into the HB^{del/+};nu/nu mice. We tested the following cell lines for tumor formation: RMG-1, a human ovarian cancer cell line; HT29, a human colon cancer cell line; MMT, a mouse breast cancer cell line; and LLC, a mouse lung cancer cell line. At 1 month after implantation, the tumors were histologically analyzed for the expression of host-derived HB-EGF by lacZ staining. Although lacZ-positive cells were scarcely observed in the corresponding normal tissues, lacZ-positive cells were detected in the stromal region of the tumors formed when RMG-1, HT29 or MMT cells were injected (Fig. 1), indicating that these cells induced HB-EGF expression in the tumor-surrounding tissues upon tumorigenesis. Immunohistochemistry for CD31, a marker of vascular endothelial cells, and SMA, a marker of cancer-associated fibroblasts (CAFs), revealed that vascular endothelial cells and/or CAFs were contained in the cell types expressing HB-EGF in the cancer stroma (Fig. 1). When LLC cells were injected, the tumor was successfully formed. However, the tumor stroma did not induce any lac-Z positive cells (Fig. 1).

Construction and characterization of the humanized mutant form of HB-EGF

CRM197 is a specific inhibitor of hHB-EGF, but does not inhibit mHB-EGF expressed in cancer-associated stromal cells in mouse cancer models. To examine whether HB-EGF expressed in stromal cells is involved in cancer progression, we generated knock-in mice expressing CRM197-inhibitable hzHB-EGF. To this end, we first constructed

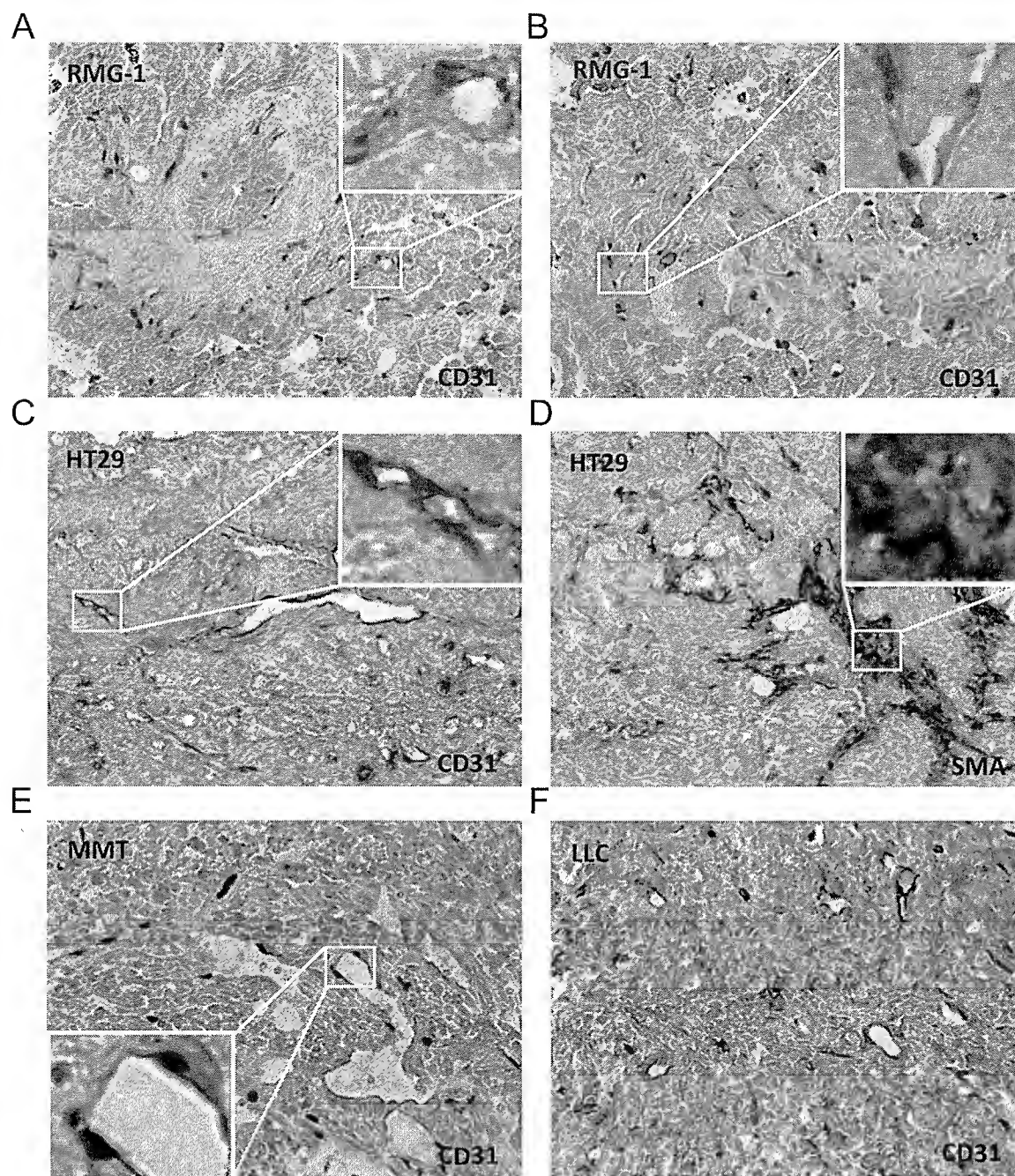


Fig. 1. HB-EGF is expressed in the cancer stroma. RMG-1, HT29, MMT and LLC cells were subcutaneously injected into HB^{del/+};nu/nu mice. Tumor sections were stained for lacZ and also stained with an anti-CD31 antibody or anti-SMA antibody, followed by counter-staining with nuclear fast red. Blue spots indicate the nuclei of lacZ-positive HB-EGF-expressing cells. CD31 and SMA are stained in brown and gray, respectively. Insets show magnified views of lacZ and CD31 double-positive cells or lacZ and SMA double-positive cells.

hzHB-EGF by swapping the EGF-like domain of mHB-EGF with the corresponding region of hHB-EGF (Fig. 2A). There are 39 and 10 amino acid substitutions within the whole molecule and the EGF-like domain, respectively, between hHB-EGF and mHB-EGF. DT and CRM197 bind

to the EGF-like domain and only the EGF-like domain is sufficient for the binding (Mitamura *et al.*, 1995; Mitamura *et al.*, 1997). Therefore, to create hzHB-EGF (*i.e.* DT-sensitive and CRM197-inhibitable), we constructed a mouse/human chimeric HB-EGF in which the EGF-like domain of

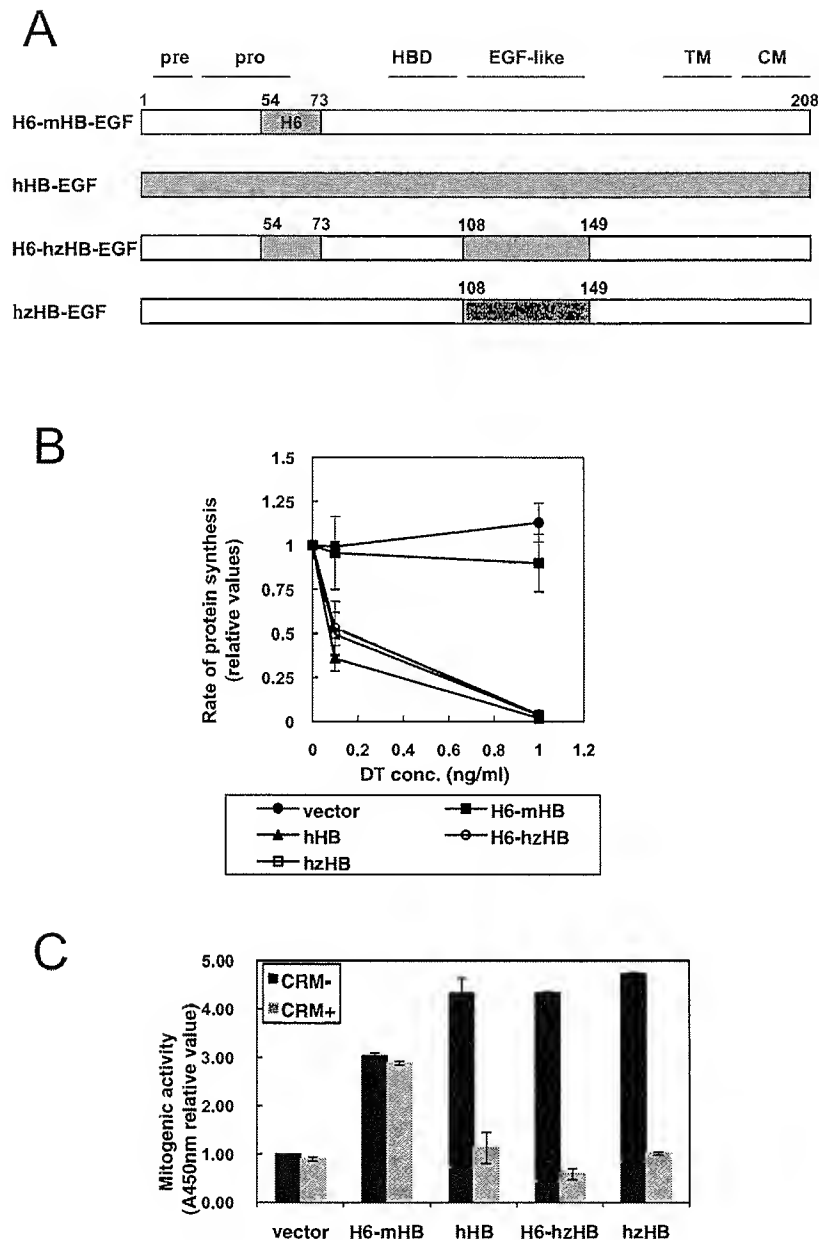


Fig. 2. Generation and characterization of hzHB-EGF knock-in mice. (A) Structures of hzHB-EGF and the related constructs. pre, signal sequence; pro, pro-domain; HBD, heparin-binding domain; TM, transmembrane domain; CM, cytosolic domain; H6, region from amino acids 54–73 of hHB-EGF recognized by the anti-H6 antibody. (B) DT sensitivity of hzHB-EGF-expressing mouse cells. hzHB-EGF, hHB-EGF, H6-hzHB-EGF and H6-mHB-EGF were separately transfected into mouse LC cells, and the DT sensitivities of the transfected cells were determined by measuring their rates of cellular protein synthesis as described in the supplementary data online. The cells expressing hzHB-EGF and H6-hzHB-EGF are sensitive to DT, similar to the cells expressing hHB-EGF. (C) Mitogenic activity of hzHB-EGF and inhibition by CRM197. Conditioned media prepared from LC cells stably expressing H6-mHB-EGF, hHB-EGF, H6-hzHB-EGF or hzHB-EGF were tested for their mitogenic activities in the DER cell system with or without 10 μ g/ml of CRM197 as described in the supplementary data online. Bars, SE.

mHB-EGF was swapped with the corresponding region of hHB-EGF. For recognition with anti-HB-EGF antibody H6, H6-mHB-EGF and H6-hzHB-EGF, in which the H6 region of mHB-EGF was swapped with the corresponding region of hHB-EGF, were also constructed (Fig. 2A). Each HB-

EGF construct was transfected into mouse LC cells and the DT sensitivities were measured by inhibition of protein synthesis (Mitamura *et al.*, 1995). Cells transfected with hzHB-EGF, H6-hzHB-EGF or hHB-EGF became equally DT-sensitive, whereas those transfected with H6-mHB-

EGF did not (Fig. 2B). DT-binding assays revealed that the K_a value of hzHB-EGF for DT was $3.9 \times 10^8 \text{ M}^{-1}$, and similar to a previously reported value for hHB-EGF ($3.6 \times 10^8 \text{ M}^{-1}$) (Mitamura *et al.*, 1995). More importantly, hzHB-EGF exhibited similar degrees of mitogenic activity to hHB-EGF and mHB-EGF, and CRM197 inhibited the mitogenic activity of hzHB-EGF similarly to that of hHB-EGF (Fig. 2C).

Generation of the knock-in mice expressing hzHB-EGF

Using the hzHB-EGF construct, hzHB-EGF knock-in (HB^{hz}) mice were generated by a gene replacement strategy that replaced the mHB-EGF gene with hzHB-EGF (Fig. 3). The targeting vector contained the mHB-EGF cDNA flanked by loxP sites linked to the hzHB-EGF cDNA (Fig. 3). This vector was introduced into mouse ES cells to generate chimeric mice carrying the HB^{hz-flox} allele. Homologous recombination in ES cells was confirmed by Southern blot analysis (Fig. 4A). Chimeric mice were bred with C57BL/

6J mice to produce heterozygous mice (HB^{hz-flox/+}). Homozygous (HB^{hz-flox/hz-flox}) mice were identified by PCR analysis (data not shown). To generate mice expressing the hzHB-EGF gene systemically, HB^{hz-flox/+} mice were crossed with CAG-Cre transgenic mice. Cre-mediated recombination was detected by PCR analysis (Fig. 4B). To confirm the expression of hzHB-EGF in HB^{hz/hz} mice, RT-PCR analysis was performed (Fig. 4C). To detect the expression of HB-EGF in this assay more easily, the mouse skins were treated with tRA (Yamazaki *et al.*, 2003). After Cre-mediated recombination, the expression of mHB-EGF was eliminated and alternative expressions of hzHB-EGF and GFP were detected. DT sensitivity of HB^{hz/hz} mice was also confirmed (Fig. 5). No overt abnormalities, including lethality and infertility, were observed in the HB^{hz/hz} mice, at least within 10 months after birth.

It should be noted that HB^{hz-flox/hz-flox} mice unexpectedly showed a leaky expression of hzHB-EGF as well as mHB-EGF and were therefore sensitive to DT (data not shown). Consequently, the generated HB^{hz-flox/hz-flox} mice are not

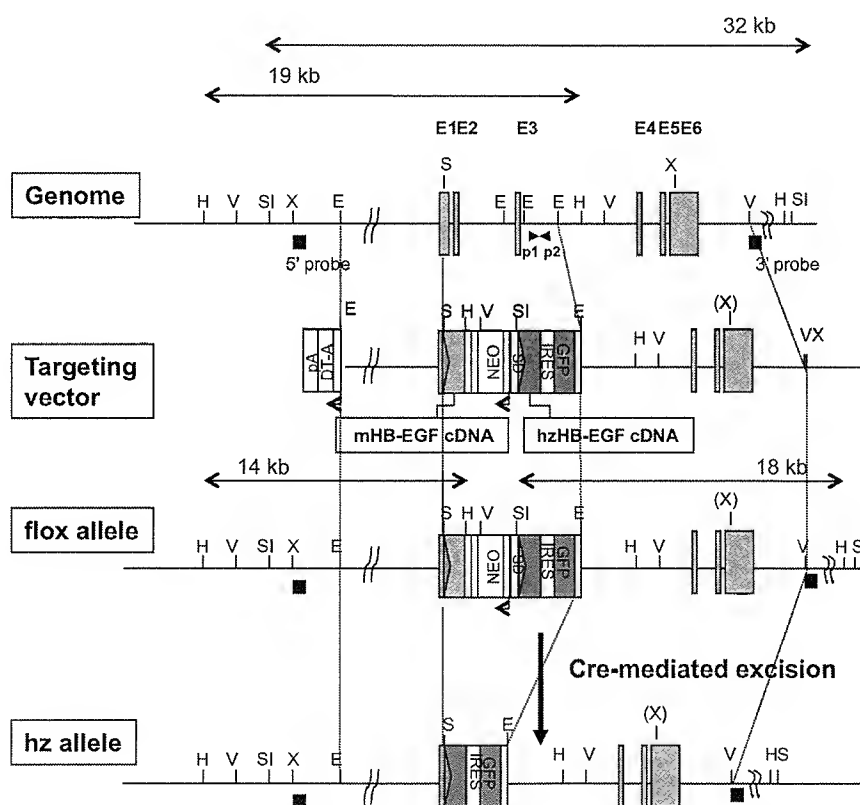


Fig. 3. Gene-targeting strategy for the generation of hzHB-EGF knock-in mice. A loxP-flanked mHB-EGF cDNA with the neomycin-resistance gene (neo) and intron 5 of the mHB-EGF gene as a splicing donor site (SD) was fused to the first exon of the mHB-EGF gene. The hzHB-EGF cDNA linked to the GFP cDNA via the internal ribosome entry site (IRES) was inserted downstream of the mHB-EGF cDNA. The targeting vector also contained the DT A-fragment (DT-A) gene. Cre-mediated recombination resulted in the deletion of the mHB-EGF cDNA and the neo cassette. Instead, hzHB-EGF and the GFP gene were expressed. Exon sequences and the loxP site are shown as gray boxes and triangles, respectively. Probes for a 5'-arm and 3'-arm are shown as black boxes. Primers for p1 and p2 are shown as arrowheads. H, *HindIII*; V, *EcoRV*; SI, *SpeI*; X, *XhoI*; E, *EcoRI*; S, *SacII*.

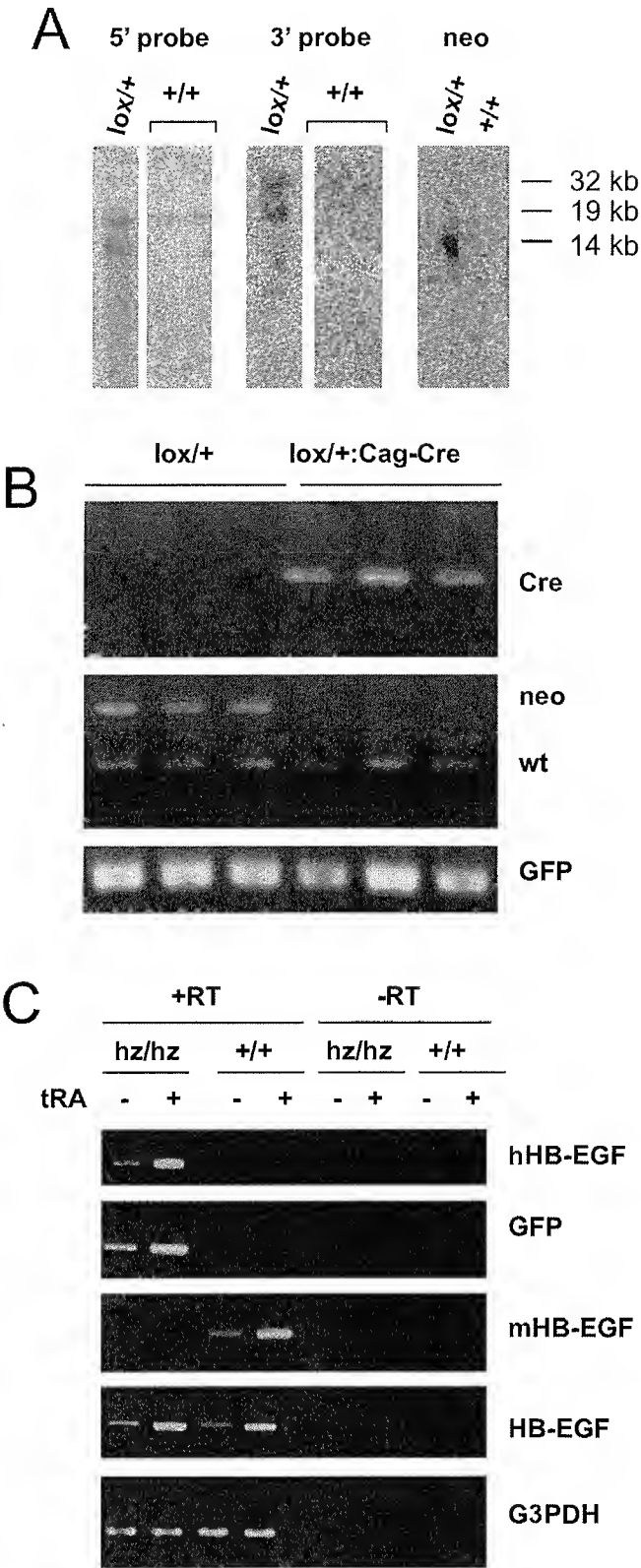


Fig. 4.

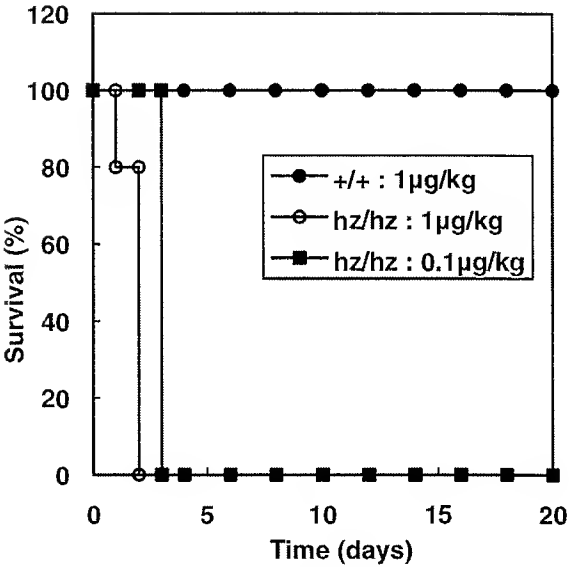


Fig. 5. DT sensitivity of hzHB-EGF knock-in mice. Survival curves of wild-type (+/+) and HB^{hz/hz} (hz/hz) mice intraperitoneally injected with DT at various doses. All mice were injected with DT at 9–10 weeks of age (n=5).

appropriate for conditional expression of hzHB-EGF in a tissue-specific manner.

Stromal HB-EGF contributes to tumor growth

We used the generated HB^{hz/hz} mice to examine whether

Fig. 4. Characterization of hzHB-EGF knock-in mice. (A) Southern blot analysis of homologous recombination in ES cells. The genomic DNA was digested with *Hind*III for hybridization with the 5' probe or *Spe*I for hybridization with the 3' probe. The 5' probe yields a 19-kb fragment from the wild-type allele and a 14-kb fragment from the hz-flox allele, while the 3' probe yields a 32-kb fragment from the wild-type allele and an 18-kb fragment from the hz-flox allele. *Spe*I-digested DNA was also analyzed with an internal probe corresponding to a sequence of the neo cassette. As a result, a 14-kb fragment was detected from the hz-flox allele, but no fragment was detected from the wild-type allele. (B) PCR analysis of genomic DNA from adult mouse tails to confirm Cre-mediated recombination. PCR analysis was performed using primer sets for wild-type allele-specific amplification (p1 and p2), GFP cDNA amplification and neo cassette amplification. To generate mice expressing hzHB-EGF, HB^{hz-flox/+} mice were crossed with CAG-Cre transgenic mice. In the presence of Cre recombinase, the band corresponding the neo gene disappeared. (C) RT-PCR analysis of the expression of hzHB-EGF. Skins from wild-type (+/+) and HB^{hz/hz} mice (hz/hz) were treated with tRA for 4 days. Total RNA extracts from these skins were analyzed by RT-PCR using the indicated primer sets as follows: hHB-EGF, for hHB-EGF-specific amplification; mHB-EGF, for mHB-EGF-specific amplification; HB-EGF, for amplification of both human and mouse HB-EGF; GFP, for amplification of GFP; G3PDH, for amplification of G3PDH (loading control). In HB^{hz/hz} mice, the expression of mHB-EGF is eliminated and hzHB-EGF and GFP are expressed instead.

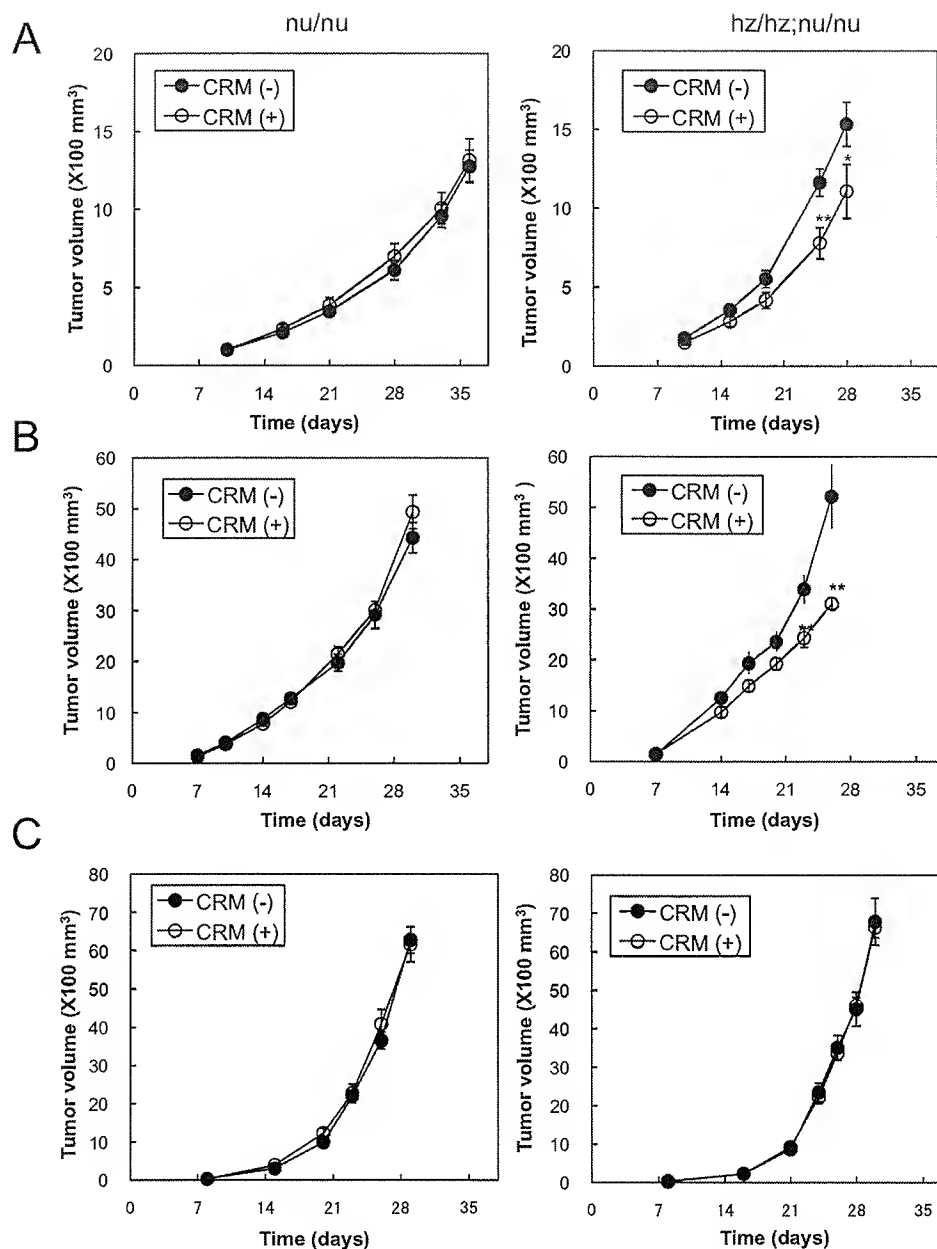


Fig. 6. Suppression of tumor growth by CRM197 administration. (A-C) HT29 (A), MTT (B) or LLC (C) cells were subcutaneously injected into nude mice (nu/nu) or HB^{hz/hz};nu/nu mice (hz/hz;nu/nu). From 1 week after the cell injection, 0.2 mg/kg of CRM197 or control saline was injected intraperitoneally every day. The tumor volumes were measured as described in Materials and Methods. Bars: SE (n=8). *p<0.05; **p<0.02.

host-derived stromal HB-EGF contributes to tumor growth. For this purpose, the following xenograft and allograft tumor models were evaluated. For the xenograft model, the human colon cancer cell line HT-29 cells were used. In this model, CRM197 should neutralize HT-29-derived hHB-EGF but not stroma-derived mHB-EGF when HT-29 cells are injected into nu/nu mice, whereas it should neutralize both HT-29-derived hHB-EGF and stroma-derived hzHB-EGF when HT-29 cells are injected into HB^{hz/hz};nu/nu mice.

HT-29 cells express HB-EGF but the expression level is much lower than those in various other cell lines, including ovarian cancer cell lines (Yotsumoto *et al.*, 2008). Consequently, we expected that the contribution of stromal HB-EGF to tumor growth would be observed more prominently using HT-29 cells than using other cell lines expressing high levels of HB-EGF. From 1 week after a subcutaneous injection of HT-29 cells, nu/nu mice and HB^{hz/hz};nu/nu mice were treated with CRM197 at 0.2 mg/kg every day.

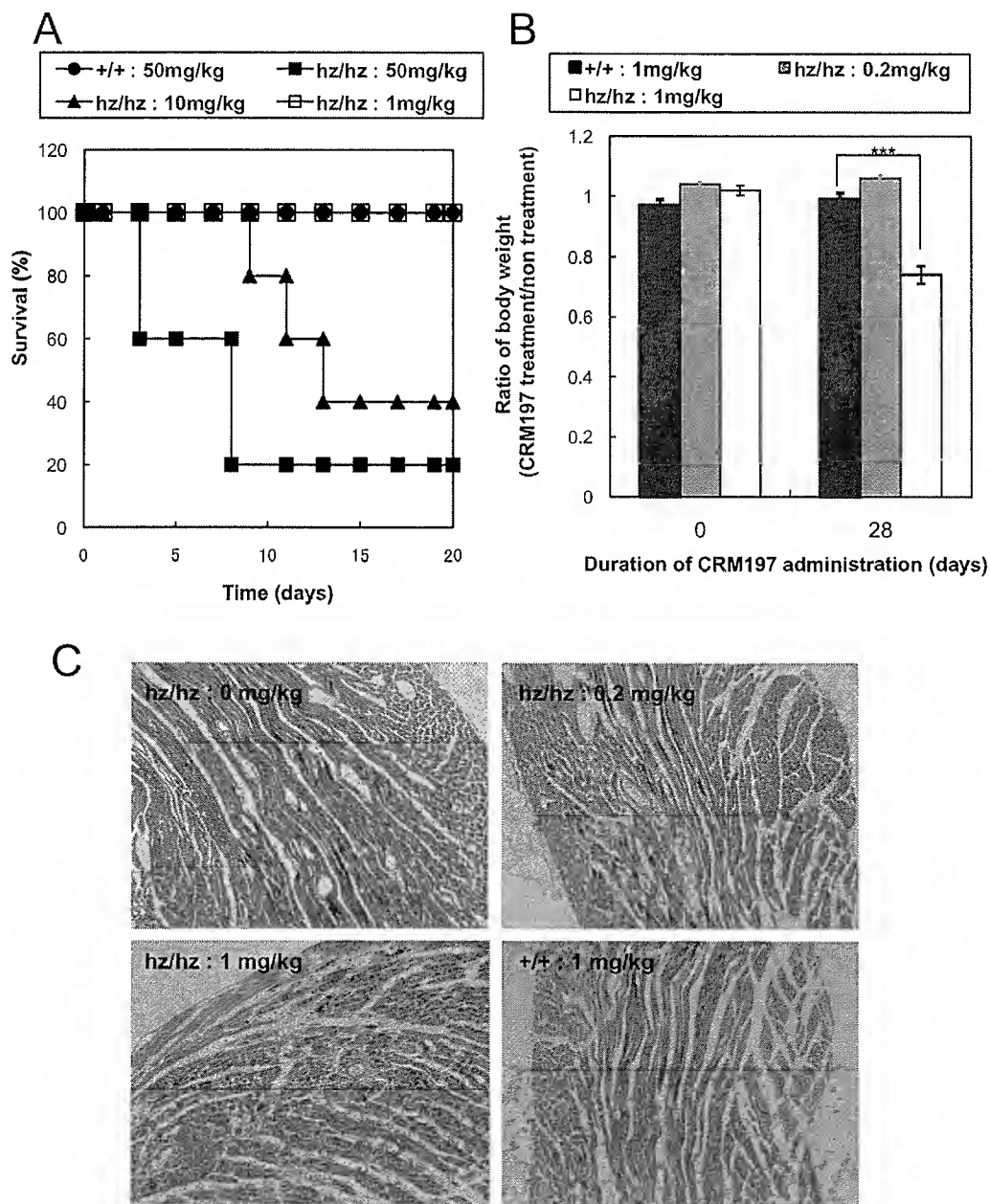


Fig. 7. Toxicology of CRM197 evaluated using hzHB-EGF knock-in mice. (A) Survival curve for a single-dose study. The indicated doses of CRM197 were intraperitoneally injected into wild-type (+/+) and HB^{hz/hz} (hz/hz) mice and their survival times were measured (n=5). (B) Effects of repeated doses of CRM197 on the body weights of mice. CRM197 at 0.2 or 1 mg/kg was intraperitoneally injected into wild-type (+/+) and HB^{hz/hz} (hz/hz) mice every day for 28 days. The average body weights at 0 and 28 days are shown as ratios to the values of untreated mice. Bars indicate the mean \pm SE (n=4). ***p<0.005. (C) Histology of HB^{hz/hz} mice treated with repeated doses of CRM197. CRM197 at 0.2 or 1 mg/kg was intraperitoneally injected into wild-type (+/+) and HB^{hz/hz} (hz/hz) mice every day for 28 days. The hearts were then removed and sections were subjected to Azan-Mallory staining. Repeated doses of CRM197 at 1 mg/kg caused fibrosis of the cardiac muscle.

CRM197 significantly suppressed the tumor growth in HB^{hz/hz};nu/nu mice but did not have this effect in nu/nu mice when the tumor growths were compared between the mice with and without CRM197 treatment (Fig. 6A). These results suggested that HB-EGF derived from the host

stroma predominantly contributed to the tumor growth of HT-29 cells, rather than the HB-EGF derived from the HT-29 cells themselves.

To further elucidate whether the host stroma-derived HB-EGF contributed to the tumor growth, we used allograft

models in which mouse carcinoma cell line MMT and LLC cells were injected subcutaneously into nu/nu mice and HB^{h_z/h_z};nu/nu mice, followed by administration of CRM197. In these models, CRM197 should not neutralize either cancer cell-derived mHB-EGF or stroma-derived mHB-EGF when the cells are injected into nu/nu mice, whereas it should only neutralize stroma-derived hzHB-EGF when the cells are injected into HB^{h_z/h_z};nu/nu mice. While CRM197 did not inhibit the tumor growth of MMT cells in nu/nu mice, it significantly suppressed the tumor growth of MMT cells in HB^{h_z/h_z};nu/nu mice (Fig. 6B). MMT cells induced HB-EGF expression in the cancer-associated stroma, whereas LLC cells did not (Fig. 1). Consistent with the loss of HB-EGF expression in the stromal region, tumors derived from LLC cells were not suppressed by CRM197 in HB^{h_z/h_z};nu/nu mice, similar to the case for nu/nu mice (Fig. 6C). These results indicate that HB-EGF expressed in the cancer stroma plays a significant role in tumor growth, either directly or indirectly. Although further studies are required to clarify the role of stromal HB-EGF, we can nevertheless conclude that HB-EGF expressed in the cancer stroma could represent a potential molecular target for future cancer therapeutic strategies.

Application of HB^{h_z/h_z} mice to physiological and pharmacological studies

The generated HB^{h_z/h_z} mice will be useful for pharmacological studies of therapeutic agents targeting hHB-EGF. The clinical development of CRM197 as an anticancer drug is in progress. We have shown in the present study that HB-EGF in the tumor stroma also contributes to tumor growth. Therefore, the knock-in mice would be more appropriate for evaluating the tumor-suppressive effects of CRM197 than conventional xenograft models using nude mice. The knock-in mice can also be used for evaluating the side effects of CRM197. CRM197 possesses a subtle toxicity (less than 10⁻⁶ of the toxicity of DT) (Kageyama *et al.*, 2007). Single-dose toxicology tests showed that administration of CRM197 at high doses (greater than 10 mg/kg) resulted in death (Fig. 7A), while repeated-dose tests revealed that daily administration of CRM197 at 1 mg/kg to HB^{h_z/h_z} mice caused body weight loss (Fig. 7B) and fibrosis of the cardiac muscle (Fig. 7C), although no overt abnormalities were observed in other tissues including the liver, kidney and brain (data not shown). Therefore, use of HB^{h_z/h_z} mice enables evaluations of the efficacy and toxicity of CRM197, and possibly other therapeutic agents targeting HB-EGF, such as antibody-based drugs, in the same mice.

HB-EGF is widely involved in physiological and pathological processes in the body. Although HB-EGF-null mice are available, these null mice show severe phenotypes in the heart and other tissues, and most of the mice die in the neonatal stage. HB^{h_z/h_z} mice will be useful for future studies examining the roles of HB-EGF in the above-mentioned

processes in combination with CRM197 or anti-HB-EGF antibodies.

Acknowledgments. We wish to thank M. Hamaoka, A. Kawai and Y. Esaki for technical assistance. The present study was supported in part by Grant-in-Aid 16207014 from the Ministry of Education, Culture, Sports, Science and Technology of Japan (to E. M.).

References

- Bhowmick, N.A., Neilson, E.G., and Moses, H.L. 2004. Stromal fibroblasts in cancer initiation and progression. *Nature*, **432**: 332–337.
- Bissery, M.C., Guenard, D., Gueritte-Voegelein, F., and Lavelle, F. 1991. Experimental antitumor activity of taxotere (RP 56976, NSC 628503), a taxol analogue. *Cancer Res.*, **51**: 4845–4852.
- Bos, P.D., Zhang, X.H., Nadal, C., Shu, W., Gomis, R.R., Nguyen, D.X., Minn, A.J., van de Vijver, M.J., Gerald, W.L., Foekens, J.A., and Massague, J. 2009. Genes that mediate breast cancer metastasis to the brain. *Nature*, **459**: 1005–1009.
- Folkman, J. and Shing, Y. 1992. Angiogenesis. *J. Biol. Chem.*, **267**: 10931–10934.
- Goishi, K., Higashiyama, S., Klagsbrun, M., Nakano, N., Umata, T., Ishikawa, M., Mekada, E., and Taniguchi, N. 1995. Phorbol ester induces the rapid processing of cell surface heparin-binding EGF-like growth factor: conversion from juxtacrine to paracrine growth factor activity. *Mol. Biol. Cell*, **6**: 967–980.
- Higashiyama, S., Abraham, J.A., Miller, J., Fiddes, J.C., and Klagsbrun, M. 1991. A heparin-binding growth factor secreted by macrophage-like cells that is related to EGF. *Science*, **251**: 936–939.
- Higashiyama, S., Abraham, J.A., and Klagsbrun, M. 1993. Heparin-binding EGF-like growth factor stimulation of smooth muscle cell migration: dependence on interactions with cell surface heparan sulfate. *J. Cell Biol.*, **122**: 933–940.
- Iwamoto, R., Higashiyama, S., Mitamura, T., Taniguchi, N., Klagsbrun, M., and Mekada, E. 1994. Heparin-binding EGF-like growth factor, which acts as the diphtheria toxin receptor, forms a complex with membrane protein DRAP27/CD9, which up-regulates functional receptors and diphtheria toxin sensitivity. *EMBO J.*, **13**: 2322–2330.
- Iwamoto, R., Yamazaki, S., Asakura, M., Takashima, S., Hasuwa, H., Miyado, K., Adachi, S., Kitakaze, M., Hashimoto, K., Raab, G., Nanba, D., Higashiyama, S., Hori, M., Klagsbrun, M., and Mekada, E. 2003. Heparin-binding EGF-like growth factor and ErbB signaling is essential for heart function. *Proc. Natl. Acad. Sci. USA*, **100**: 3221–3226.
- Kageyama, T., Ohishi, M., Miyamoto, S., Mizushima, H., Iwamoto, R., and Mekada, E. 2007. Diphtheria toxin mutant CRM197 possesses weak EF2-ADP-ribosyl activity that potentiates its anti-tumorigenic activity. *J. Biochem.*, **142**: 95–104.
- Kalluri, R. and Zeisberg, M. 2006. Fibroblasts in cancer. *Nat. Rev. Cancer*, **6**: 392–401.
- Mitamura, T., Higashiyama, S., Taniguchi, N., Klagsbrun, M., and Mekada, E. 1995. Diphtheria toxin binds to the epidermal growth factor (EGF)-like domain of human heparin-binding EGF-like growth factor/diphtheria toxin receptor and inhibits specifically its mitogenic activity. *J. Biol. Chem.*, **270**: 1015–1019.
- Mitamura, T., Umata, T., Nakano, F., Shishido, Y., Toyoda, T., Itai, A., Kimura, H., and Mekada, E. 1997. Structure-function analysis of the diphtheria toxin receptor toxin binding site by site-directed mutagenesis. *J. Biol. Chem.*, **272**: 27084–27090.
- Miyamoto, S., Hirata, M., Yamazaki, A., Kageyama, T., Hasuwa, H., Mizushima, H., Tanaka, Y., Yagi, H., Sonoda, K., Kai, M., Kanoh, H., Nakano, H., and Mekada, E. 2004. Heparin-binding EGF-like growth factor is a promising target for ovarian cancer therapy. *Cancer Res.*, **64**: 5720–5727.

- Miyamoto, S., Yagi, H., Yotsumoto, F., Kawarabayashi, T., and Mekada, E. 2006. Heparin-binding epidermal growth factor-like growth factor as a novel targeting molecule for cancer therapy. *Cancer Sci.*, **97**: 341–347.
- Mueller, M.M. and Fusenig, N.E. 2004. Friends or foes — bipolar effects of the tumour stroma in cancer. *Nat. Rev. Cancer*, **4**: 839–849.
- Normanno, N., Bianco, C., De Luca, A., Maiello, M.R., and Salomon, D.S. 2003. Target-based agents against ErbB receptors and their ligands: a novel approach to cancer treatment. *Endocr. Relat. Cancer*, **10**: 1–21.
- Ongusaha, P.P., Kwak, J.C., Zwible, A.J., Macip, S., Higashiyama, S., Taniguchi, N., Fang, L., and Lee, S.W. 2004. HB-EGF is a potent inducer of tumor growth and angiogenesis. *Cancer Res.*, **64**: 5283–5290.
- Raab, G. and Klagsbrun, M. 1997. Heparin-binding EGF-like growth factor. *Biochim. Biophys. Acta*, **1333**: F179–199.
- Sakai, K. and Miyazaki, J. 1997. A transgenic mouse line that retains Cre recombinase activity in mature oocytes irrespective of the cre transgene transmission. *Biochem. Biophys. Res. Commun.*, **237**: 318–324.
- Takazaki, R., Shishido, Y., Iwamoto, R., and Mekada, E. 2004. Suppression of the biological activities of the epidermal growth factor (EGF)-like domain by the heparin-binding domain of heparin-binding EGF-like growth factor. *J. Biol. Chem.*, **279**: 47335–47343.
- Tlsty, T.D. and Coussens, L.M. 2006. Tumor stroma and regulation of cancer development. *Annu. Rev. Pathol.*, **1**: 119–150.
- Uchida, T., Pappenheimer, A.M.J., and Greany, R. 1973. Diphtheria toxin and related proteins. I. Isolation and some properties of mutant proteins serologically related to diphtheria toxin. *J. Biol. Chem.*, **248**: 3838–3844.
- Umata, T., Moriyama, Y., Futai, M., and Mekada, E. 1990. The cytotoxic action of diphtheria toxin and its degradation in intact Vero cells are inhibited by bafilomycin A1, a specific inhibitor of vacuolar-type H(+)-ATPase. *J. Biol. Chem.*, **265**: 21940–21945.
- Yamazaki, S., Iwamoto, R., Saeki, K., Asakura, M., Takashima, S., Yamazaki, A., Kimura, R., Mizushima, H., Moribe, H., Higashiyama, S., Endoh, M., Kaneda, Y., Takagi, S., Itami, S., Takeda, N., Yamada, G., and Mekada, E. 2003. Mice with defects in HB-EGF ectodomain shedding show severe developmental abnormalities. *J. Cell Biol.*, **163**: 469–475.
- Yotsumoto, F., Yagi, H., Suzuki, S.O., Oki, E., Tsujioka, H., Hachisuga, T., Sonoda, K., Kawarabayashi, T., Mekada, E., and Miyamoto, S. 2008. Validation of HB-EGF and amphiregulin as targets for human cancer therapy. *Biochem. Biophys. Res. Commun.*, **365**: 555–561.

(Received for publication, December 4, 2009, accepted, January 14, 2010
and published online, February 27, 2010)

EGF Receptor Antagonism Improves Survival in a Murine Model of Pancreatic Adenocarcinoma¹

Alan J. Durkin, M.D.,*† Dana A. Osborne, M.D.,* Timothy J. Yeatman, M.D., F.A.C.S.,†
Alexander S. Rosemurgy, M.D., F.A.C.S.,* Cindy Armstrong, B.A.,*
and Emmanuel E. Zervos, M.D., F.A.C.S.*†²

*University of South Florida College of Medicine, Department of Surgery, Tampa General Hospital, Digestive Disorders Center, Tampa, Florida 33612; and †GI Tumor Program, H. Lee Moffitt Cancer Center and Research Institute, Tampa, Florida

Submitted for publication December 15, 2005

Introduction. The purpose of this study was to determine whether inhibition of the epidermal growth factor receptor (EGFR) is a plausible therapeutic strategy in pancreatic cancer.

Methods. A human pancreatic cancer cell line (HPAC) was evaluated for the presence of EGFR with rtPCR and immunohistochemistry. Cells were grown in the presence of either 50 or 100 μM of erlotinib (EGFRI) for 72 hours and evaluated using the 3-(4,5-dimethylthiazol-2-yl)-2,5-diphenyltetrazolium bromide (MTT) assay. Eighty-six athymic nude/nude mice underwent orthotopic implantation of 10^7 HPAC cells and were blindly randomized into four groups: (1) Control; (2) Batimastat, a matrix metalloproteinase inhibitor (MMPI) at 400 ng/ml qod; (3) EGFRI at 100 mg/kg qd; and (4) MMPI and EGFRI (both). *In vitro* and *in vivo* effects of EGFRI with and without MMPI were compared.

Results. HPAC demonstrated high levels of expression of both the EGFR gene and the gene product. *In vitro*, both doses of EGFRI significantly reduced proliferation of HPAC at 48 (50 μM : 1.15 ± 0.05 [st dev] versus 0.63 ± 0.09 abs, $P < 0.001$) and 72 h (50 μM : 1.48 ± 0.09 versus 0.73 ± 0.05 abs, $P < 0.001$, paired Student's *t*-test). *In vivo*, each treatment group demonstrated a significant survival advantage ($P = 0.0002$ group 2, $P = 0.0001$ group 3, $P = 0.012$ group 4, log rank test) over controls. Mice treated with EGFRI showed reduced tumor implantation, size, weight, metastatic potential,

and jaundice as compared to controls and MMPI-treated mice (all $P < 0.05$, Fisher's exact test).

Conclusion. EGF receptor antagonism is not only a plausible therapy for treatment of ductal adenocarcinoma of the pancreas, but is also superior to matrix metalloproteinase inhibition alone or in combination. © 2006 Elsevier Inc. All rights reserved.

Key Words: EGF receptor; pancreatic adenocarcinoma; athymic mouse; immunohistochemistry.

INTRODUCTION

Effective treatment of pancreatic adenocarcinoma remains a major challenge in modern medicine. While surgical therapy offers patients with this disease hope for long-term survival or cure, over 80% of patients are ineligible for resection at presentation [1–3]. Furthermore, recurrent disease following curative resection confers an abysmal prognosis as our current chemotherapeutic regimens predictably fail in achieving a survival benefit in this patient population, while succeeding in potentially unnecessary systemic toxicity [4].

The expansion and distribution of genetic technology has offered new insight into pancreatic adenocarcinoma. Numerous investigators have demonstrated that pancreatic adenocarcinomas, as well as other gastrointestinal tumors, show significant expression of the epidermal growth factor receptor (EGFR) gene and gene product [2–9]. The EGF receptor is a transmembrane tyrosine kinase protein that has been shown to be overexpressed in as many as 80% of pancreatic ductal adenocarcinomas [8, 9]. Stimulation of the EGF receptor in cancer cells *in vitro* results in the activation of multiple intracellular signaling cascades, which increase cellular proliferation and prevent programmed cell death [10–12].

¹ Presented at the 90th Annual American College of Surgeons Surgical Forum—October 22nd, 2004.

² To whom correspondence and reprint requests should be addressed at Tampa General Hospital, Digestive Disorders Center, Room F-145, P.O. Box 1289, Tampa, Florida 33601. E-mail: ezervos@hsc.usf.edu.

These findings support the EGF receptor as a potential therapeutic target in the treatment of epithelial-derived solid tumors that express it and have resulted in the recent development of novel, innovative strategies for inhibition of this receptor, including monoclonal antibodies and small molecule tyrosine kinase inhibitors specific for the EGF receptor. We have previously characterized EGF receptor gene and protein expression in multiple pancreatic cancer cell lines and have shown that Erlotinib® (OSI-774, OSI Pharmaceuticals, Melville, NY), a small molecule tyrosine kinase inhibitor, inhibits *in vitro* proliferation of these cell lines, all of which express the EGFR [13]. The purpose of this investigation was to determine the effect Erlotinib (EGFRI), on cellular proliferation *in vitro* and tumorigenesis using a cachexia model *in vivo* in a pancreatic cancer cell line known to express the EGF receptor using an established orthotopic model [14]. This model has been established by our laboratory and is known to result in consistent, predictable life expectancy in untreated animals at 60 days [13–18]. In this study, we hypothesized that EGF receptor inhibition would inhibit cellular growth *in vitro* and, as such, generate a survival benefit *in vivo*. We further sought to contrast Erlotinib's *in vivo* activity against and in combination with BB-94, a matrix metalloproteinase inhibitor upon which the *in vivo* model was established.

METHODS

Cell Culture

Human pancreatic adenocarcinoma (HPAC; ATCC No. CRL-2119), a moderately differentiated pancreatic cancer cell line with metastatic potential, was grown to near confluence in Falcon disposable 100 × 20 mm tissue culture dishes (PGC Scientifics, Baltimore, MD). Media consisted of DMEM-F12 (Gibco, Carlsbad, CA) with 5% fetal bovine serum (Atlanta Biologicals, Lawrenceville, GA) and the following additives (Sigma-Aldrich, St. Louis, MO): insulin (1 mg/500 ml), transferrin (5 mg/500 ml), hydrocortisone (20 µg/500 ml), EGF (5 µg/500 ml), and penicillin/streptomycin solution (5 mg/500 ml).

EGF Receptor Gene Expression

Total RNA was harvested from near confluent dishes of HPAC. One million HPAC cells were scraped from 100 × 20 mm plates and then washed before the addition of 5 ml Trizol solution (Gibco-BRL). The solution was mixed for 20 s and then incubated at room temperature for 5 min. Following the addition of 1 ml chloroform, the solution was mixed and incubated at room temperature for 2 min. It was then centrifuged at 7200 g for 15 min at 4°C. RNA was precipitated from the supernatant using 80% ethanol and purified using RNeasy Midi Kit (Qiagen, Inc., Valencia, CA) according to the manufacturer's instructions.

A total of 500 ng of pure, total RNA was transcribed using AMV Reverse Transcriptase (Roche Applied Science, Indianapolis, IN). The resultant cDNA was then probed for EGF receptor gene expression and the housekeeping control gene, glucose phosphate isomerase (GPI). PCR was run for 33 cycles using HotMaster Taq (Eppendorf Corp., Westbury, NY), denaturing at 95°C for 35 s, annealing at 55°C for 25 s, and extending at 72°C for 35 s. Reactions were under-

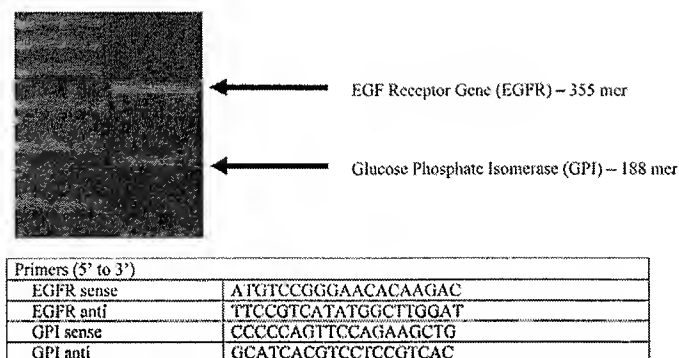


FIG. 1. Semiquantitative rtPCR for the EGF receptor gene (target gene), and glucose phosphate isomerase (control gene).

taken with 2 µl cDNA in a total volume of 26 µl and run on a 2% agarose gel with ethidium bromide for visualization (0.4 µg/ml). Primer sequences are listed in Fig. 1.

EGF Receptor Protein Expression

For each cell line, a near confluent 100 × 20 mm dish was washed with 10 ml cold PBS twice, and cells were then lifted using 1 ml 0.1% trypsin-EDTA. Following dislodgement, cells were suspended in PBS with 20% fetal bovine serum and underwent centrifugation at 1500 g for 3 min. The supernatant was aspirated, and the cells were resuspended in 1 ml of 20% FBS/PBS solution. At a 1:10 dilution, cells were counted via hemocytometer, and the volume necessary for suspending 50,000 cells in 250 µl of solution was calculated and placed on a pre-etched, double-positive Shandon slide. The slide was then centrifuged for 5 min at 570 rpm, fixed in 4% paraformaldehyde for 10 min, rinsed with nonsterile PBS, air-dried, and placed at -80°C overnight.

Immunostaining was undertaken using a rabbit polyclonal anti-EGF receptor antibody targeting the carboxy-terminus of human EGF receptor (Santa Cruz Biotech, Santa Cruz, CA). Staining was carried out using a BenchMark IHC/ISH automated staining module (Ventana Medical Systems, Tucson, AZ) according to the manufacturer's recommendations. Antibody was diluted to a 1:100 solution using Antibody Diluent (Ventana Medical Systems). An incubation time of 32 min was used. Cells were subsequently counterstained using hematoxylin, coverslipped, and graded by an independent pathologist using the scoring system described by Allred *et al.* [19].

EGFR Antagonism *In Vitro*

At near confluence, cell lines were harvested using 0.1% trypsin-EDTA. Cells were centrifuged, diluted 1:10, and counted using a Coulter counter (Beckman Coulter Corp., Model Z1). Using sterile 96-well plates, 2500 HPAC cells were plated per well. Cells were then grown for 72 h in the presence of the following: (1) control vehicle (0.1% DMSO); (2) 50 µM EGFRI in 0.1% DMSO; and (3) 100 µM EGFRI in 0.1% DMSO. Cellular proliferation was determined by CellTiter 96 assay at 24-h intervals for a total of 72 h. At 24-h intervals, 15 µl of 3-[4,5-dimethylthiazol-2-yl]-2,5-diphenyltetrazolium bromide (MTT) solution (Promega, Madison, WI) was added to each well. This solution was then incubated for 4 h at 37°C in a 5% CO₂ environment. Next, 100 µl of stop solution was added and allowed to incubate overnight. Plates were then separately mixed and read at 570 nm wavelength using a Dynatech MR5000 plate reader (Dynatech Laboratories, Inc., Chantilly, VA). Absorbance (abs) was recorded to the third decimal point, and cellular growth curves were generated and compared to control at two time points, 48 and 72 h. Cells were plated in four wells each, and the experiments were carried out twice to confirm the results.

EGFR Antagonism *In Vivo*

With full approval from the Laboratory Medical Ethics Committee at the University of South Florida, 86 NCI athymic nude/nude mice were obtained from the NCI Biotech Corporation. Mice were allowed to acclimate to their surroundings for 7 days. Subsequently, mice were anesthetized using 0.02 mg/kg intraperitoneal pentobarbital. A midline abdominal incision was used for exposure of the peritoneal cavity. The greater curvature of the stomach was identified and carefully delivered into the wound. Identification of the pancreas was done visually, and ten million HPAC cells suspended in a volume of 0.1 ml Hank's balanced salt solution (HBSS, Gibco, Lot no. 1124589) were injected into the peripancreatic space using a 27-gauge needle.

Prior to surgery, all animals were weighed to determine their baseline body weight. Individual animal weights were determined at 7-day intervals throughout the course of the study. Our study used universally accepted criteria for morbidity, and animals determined to be in a premonitory state were euthanatized via carbon dioxide asphyxiation. The decision to euthanize animals was made jointly by the principal investigator and the animal care coordinator at the James A. Haley Veterans Administration vivarium. Endpoints for compassionate euthanasia included the following: (1) cachexia (defined as body weight less than 10% baseline); (2) ataxia; (3) respiratory rate <15 breaths per min as evidence of respiratory distress; (4) cyanosis; (5) profound loss of skin turgor; and (6) persistent isolation from cage mates with presence of skin lesions. The date of euthanasia of the animals was reported as the date of death from disease in the survival analysis.

Secondary endpoints included jaundice, ascites, tumor weight, and volume. Jaundice was determined by clinical examination of the skin. Ascites were defined as a protuberant abdomen with aspiration of 1 ml or greater of free, serous abdominal fluid prior to treatment. All tumors were excised immediately following death, weighed and measured, and then snap-frozen in liquid nitrogen. Tumor volume (TV) was calculated by the following formula: $TV = 0.5ab^2$, where a is the length in mm, and b is the width in mm.

Mice were allowed to recover for 7 days after tumor implantation. During this period, all mice were placed in a single cage and randomly selected to be placed in one of four subsequent cages: control, EGFR, matrix metalloproteinase inhibitor (MMPI), or EGFR plus MMPI (both). Thirteen mice were used as control animals, 18 MMPI, 17 EGFR, and 19 received both treatments. Numbers in each group reflect the number of animals surviving tumor implantation and either dying of tumor-related causes or surviving to the end of the study.

Batimastat was used to institute MMPI. Batimastat (British Biomedical Corp.) was suction-extracted from gel capsules and diluted in medium-chain triglyceride (MCT) oil to a concentration of 400 ng/kg. Drug was administered in 100 μ l increments by sterile intraperitoneal injection every other day for a total of 60 days. Erlotinib (EGFR, OSI-774, OSI Pharmaceuticals) was solubilized in captisol solution (6% weight per volume) to a concentration of 100 mg/kg. Erlotinib was delivered by sterile intraperitoneal injection at a volume of 100 μ l every day for a total of 60 days.

Both drugs were solubilized fresh on the day of injection. Mice receiving combination chemotherapy (MMPI and EGFR) received two separate injections per treatment, each of which had a volume of 100 μ l. Control mice received 100 μ l of MCT oil every other day, and 100 μ l of captisol every day by sterile intraperitoneal injection.

Statistics and Data Management

In vitro absorbance data were entered into an Excel spreadsheet (Microsoft Corp., Redmond, WA). Mean absorbances were compared for control *versus* each dose of EGFR using a paired Student's *t*-test as were the absorbances between the two doses of EGFR at 48 and 72 h. Data are reported as mean \pm standard deviation of absorbance. Significance was accepted when the *P* value was less than or equal to 0.05.

The risk of developing jaundice and ascites in each treatment group was compared against the control group using the Fisher's exact test. Significance again was accepted with *P* values <0.05 and is reported with 95% confidence intervals. Tumor weights and volumes between each group were compared using a paired Student's *t*-test and are reported as mean \pm standard deviation.

Survival curves were derived using the Kaplan-Meier method. Curves were compared for subgroups of animals using the log-rank test. First all four groups were compared to confirm or refute the null hypothesis: that the survival curves were not different. Next, six separate pair-wise comparisons were made using the log rank test: control *versus* EGFR, control *versus* MMPI and control *versus* both, EGFR *versus* MMPI, EGFR *versus* both, and MMPI *versus* both. *P* values for each individual pair-wise comparison are reported in the figures.

RESULTS

EGFR Expression

HPAC showed strong expression of the EGF receptor gene. EGF receptor mRNA expression is shown against the background of glucose phosphate isomerase in Fig. 1. Immunohistochemical analysis of HPAC cells showed significant receptor-specific staining for EGFR and was scored 8/8 by an independent pathologist using the Allred scoring system (Fig. 2).

In Vitro Growth Kinetics

Cellular proliferation is illustrated in Fig. 3. Proliferation was significantly inhibited with 50 μ M EGFR *versus* control at 48 h (abs: 1.2 ± 0.05 [control] *versus* 0.63 ± 0.094 , $P < 0.001$) and 72 h (1.48 ± 0.089 [control] *versus* 0.73 ± 0.047 , $P < 0.001$). Proliferation was similarly reduced with the 100 μ M dose at 48 h (1.2 ± 0.05 [control] *versus* 0.74 ± 0.156 , $P < 0.001$) and 72 h (1.48 ± 0.89 [control] *versus* 0.583 ± 0.187 , $P < 0.001$); 100 μ M EGFR was also significantly more inhibitory than 50 μ M at 72 h only (abs: 0.73 ± 0.047 [50 μ M]

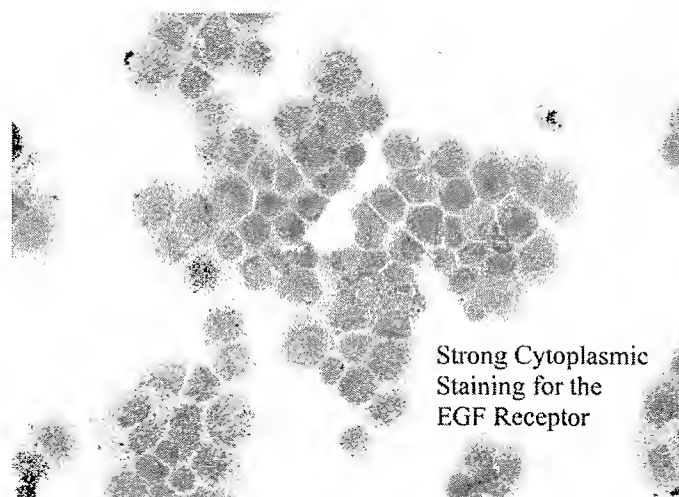


FIG. 2. Immunohistochemical staining for the EGF receptor in pancreatic cancer cells grown *in vitro*. (Color version of figure is available online.)

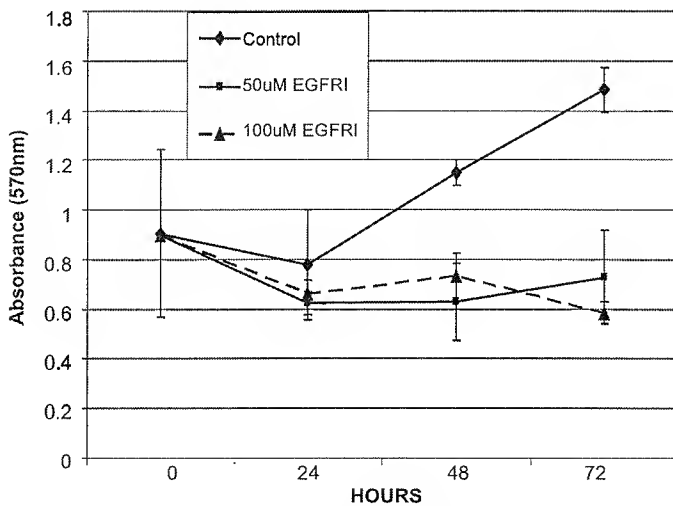


FIG. 3. *In vitro* growth kinetics of HPAC cells grown in presence of control vehicle (0.1% DMSO), 50 μ M EGFR1, and 100 μ M EGFR1. Kinetics were assessed using an MTT assay. Growth inhibition at each dose of EGFR1 was significant at 48 and 72 h ($P < 0.05$, Student's *t*-test).

versus 0.58 ± 0.187 , $P = 0.055$). Trypan blue was used to confirm cell viability independently in all treatment groups.

In Vivo Survival

The treatments used generated significant survival differences in the three groups receiving chemotherapy ($P < 0.05$, log rank test). When compared individually against the control group, each treatment demonstrated a significant survival advantage. The greatest survival advantage was seen in mice treated with EGFR1 alone ($P < 0.0001$ versus control), with 47% of those mice surviving to the predefined 60 day end point. Survival with associated P values are graphically depicted in Fig. 4. Comparatively, mice undergoing MMPI alone demonstrated a significant survival advantage, but only 11% of those mice survived the 60-day trial. Mice that received combination chemotherapy (MMPI/EGFR1) showed significant survival improvement as compared to controls, but did significantly worse than either monotherapy subset. There was no survival advantage with EGFR1 when compared to MMPI.

Secondary Endpoints

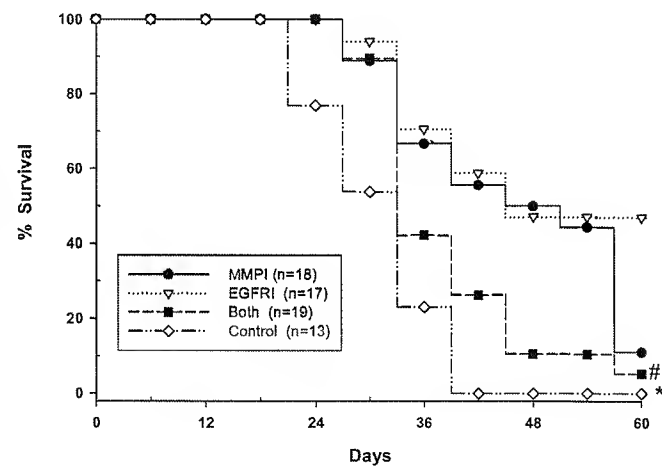
The likelihood of developing ascites or jaundice was significantly reduced in all groups receiving EGFR1 as part of their regimen, while MMPI alone reduced the incidence of ascites only (Fig. 5). Side effects most commonly seen in the MMPI group included wound complications (dehiscence requiring reclosure), while the group receiving EGFR1 had no notable side effects.

Each treatment group had significantly smaller tumors by both weight and volume, as compared to control animals. Addition of EGFR1 either alone, or with MMPI, also resulted in smaller tumors by weight when compared to MMPI alone (Fig. 6).

DISCUSSION

Effective therapy for pancreatic adenocarcinoma has, thus far, eluded both physicians and surgeons. Recent advances in genetic profiling have allowed us to identify and examine the molecular foundations of this disease. One such foundation appears to be the EGF receptor. This receptor has been demonstrated to interact with numerous intracellular pathways implicated in both the genesis and the maintenance of pancreatic adenocarcinoma [6, 13, 14, 20]. Numerous independent investigators have documented both genomic and proteomic overexpression of the EGF receptor in pancreatic adenocarcinoma as compared to normal pancreata. Taken cumulatively, these observations identify the EGF receptor as a plausible molecular target for chemotherapy [6, 13, 14, 19–25]. In response to this identification, numerous methodologies for EGF receptor antagonism have been proposed and developed in the recent literature, including the development of an entirely new class of small molecule tyrosine kinase inhibitors specific for the EGF receptor. The purpose of this investigation was to confirm overexpression of the EGF receptor in an immortalized pancreatic cell line and then to evaluate EGF receptor blockade as therapy in both an *in vitro* and an *in vivo* system.

Using semiquantitative rtPCR and immunohistochemistry, our investigation demonstrated significant



* significantly shorter survival than both ($p=0.012$); MMPI($p=0.0002$) and EGFR1($p=0.0001$)
significantly shorter than EGFR1 (0.0058); MMPI ($p=0.0554$)

FIG. 4. Kaplan-Meier survival curve demonstrating survival in four randomized groups of athymic nude mice.

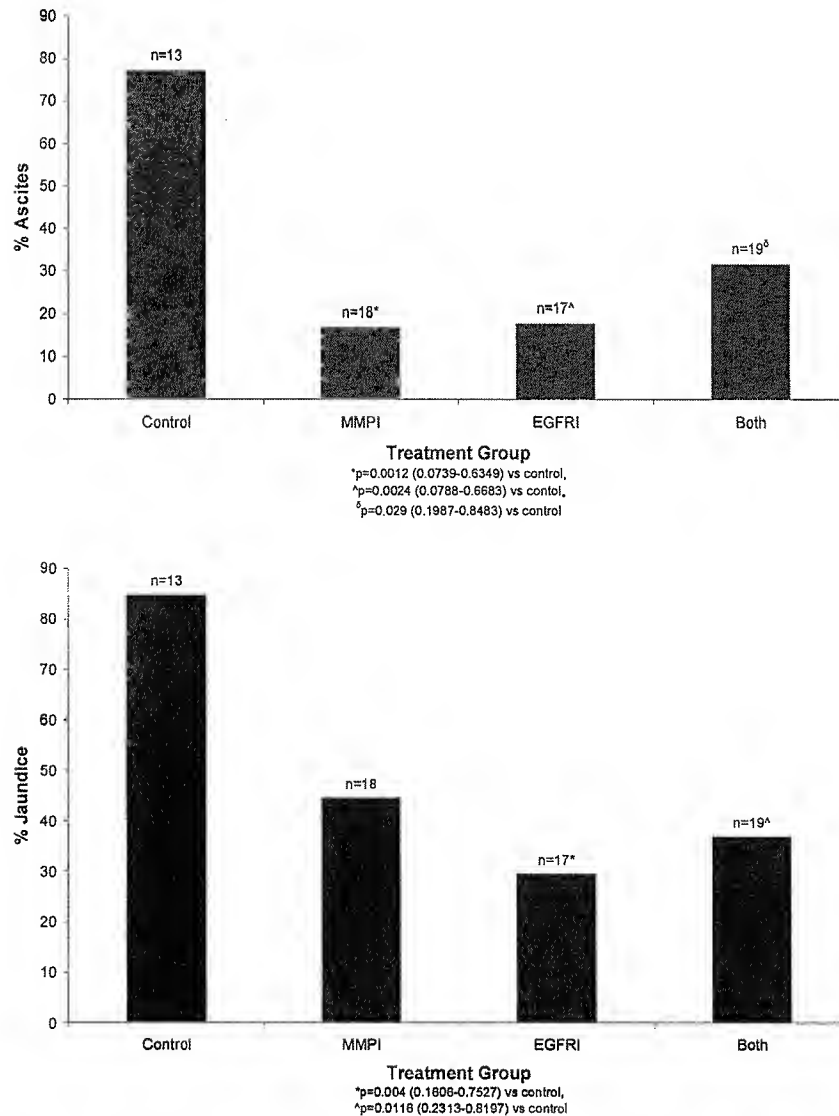


FIG. 5. Incidence of ascites and jaundice (MMPI—matrix metalloproteinase inhibition with BB-94, EGFRi-EGF receptor inhibition with erlotinib).

expression of the EGF receptor in our HPAC cell line. We isolated activated EGFR both on the cell membrane, and to a lesser extent, within the cytosol. This was not an unexpected finding. While the receptor itself is a transmembrane receptor, it does have an extracellular binding site, and an intracellular tyrosine kinase domain. This finding is consistent with other investigations, which also document significant expression of the EGF receptor in numerous types of solid, epithelial-derived gastrointestinal cancers. Subsequently, utilization of EGF receptor blockade in an *in vitro* system demonstrated statistically significant growth inhibition at both 48- and 72-h intervals as compared to controls. These results suggested that pancreatic cancer cells with significant expression of the EGF receptor could be effectively treated with EGF receptor antagonism. Other independent investigators

using multiple modalities for EGF receptor antagonism have also demonstrated reduced cellular proliferation, supporting EGF receptor antagonism as a plausible therapy for this disease. Scwab *et al.* demonstrated significant growth inhibition using the anti-EGFR monoclonal antibody IMC-225 on MDA Panc-28 cells grown *in vitro* [26]. Lee *et al.* demonstrated the efficacy of EGFR antagonism using two separate antioxidant flavonoids Quercetin and Luteolin. Their study showed significant inhibition of the EGF receptor, and a direct relationship between EGF receptor antagonism and cellular growth inhibition [27]. Cumulatively, these reports and others indicate that EGF receptor antagonism in an *in vitro* system, regardless of inhibitory method used, is an effective measure for reduction of cellular proliferation in pancreatic adenocarcinoma cells.

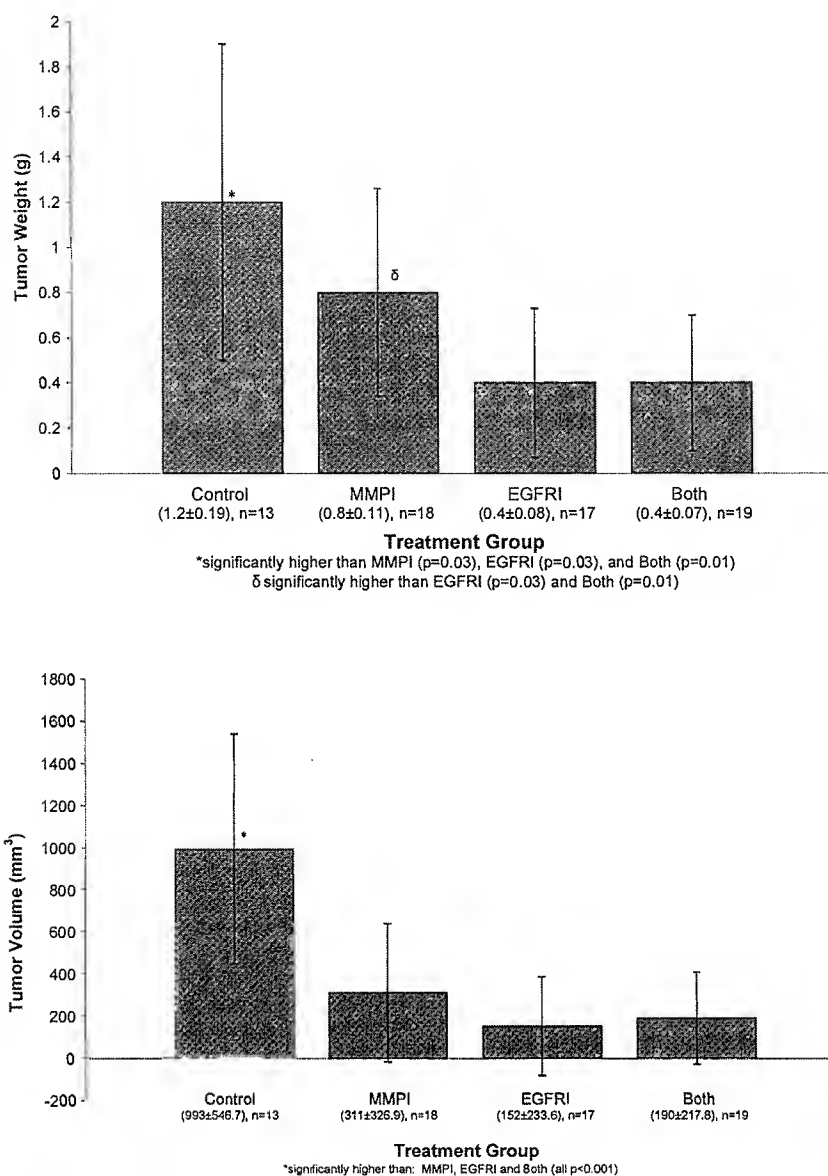


FIG. 6. Comparison of tumor weight (g) and volume (mm³) between the treatment groups.

Our murine model of pancreatic adenocarcinoma attempted to quantify the clinical potential of EGF receptor antagonism for clinical treatment. A significant survival advantage was demonstrated in mice that received EGF receptor antagonism therapy as compared to the controls. Furthermore, EGF receptor antagonism also outperformed matrix metalloproteinase inhibition in numerous clinical categories, including the incidence of jaundice, ascites, tumor weight, and tumor volume. Also, 47% of mice treated with EGFRi were alive at 60 days, as compared with only 11% of mice receiving MMPI. These results suggest, but do not confirm, that EGFRi therapy is indeed superior to MMPI treatment.

Our study did not document a synergistic effect of combination MMPI and EGFRi therapy. In fact, a de-

creased survival was noted in our combination chemotherapy cohort. Furthermore, an increase in the incidence of both ascites and jaundice in the combination chemotherapy group was noted as compared to our single-agent cohorts. Our interpretation of these results is that significant hepatic toxicity was generated by multi-agent therapy and that survival in this group was reduced due to drug-induced systemic toxicity rather than failure to effectively treat the underlying cancer. The concomitant use of MMP inhibition and EGFR inhibition, in our opinion, still represents a plausible treatment modality for pancreatic adenocarcinoma, but dose reductions of either agent or both appear to be indicated.

This study offers further evidence that inhibition of the EGF receptor is a plausible therapy for pancreatic

adenocarcinoma. Our *in vitro* and *in vivo* investigations clearly indicate that the EGF receptor remains an attractive molecular target for treatment in patients with this disease. Specifically, utilization of erlotinib, a small molecule tyrosine kinase inhibitor specific for the EGF receptor, may represent a clinically applicable and efficacious therapy for pancreatic adenocarcinoma.

ACKNOWLEDGMENTS

OSI Pharmaceuticals provided Erlotinib free of charge for the purposes of this investigation. We thank Dr. Alan B. Cantor for statistical review of the manuscript and Linda Atkinson, B.S., for provision of supplies necessary for preparation of therapeutic agents.

REFERENCES

1. Zervos EE, Rosemurgy AS, Al-Saif O, et al. Surgical management of early-stage pancreatic cancer. *Cancer Control* 2004; 11:23.
2. Kalser MH, Ellenberg SS. Pancreatic cancer. Adjuvant combined radiation and chemotherapy following curative resection. *Arch Surg* 1985;120:899.
3. Bouvet M, Gamagami RA, Gilpin EA, et al. Factors influencing survival after resection for perianapillary neoplasms. *Am J Surg* 2000;180:13.
4. Wolff RA. Exploiting molecular targets in pancreatic cancer. *Hematol Oncol Clin North Am* 2002;16:139.
5. Baselga J, Pfister D, Cooper MR, et al. Phase I studies of anti-epidermal growth factor receptor chimeric antibody C225 alone and in combination with cisplatin. *J Clin Oncol* 2000;18:904.
6. Xiong HQ, Abbruzzese JL. Epidermal growth factor receptor-targeted therapy for pancreatic cancer. *Semin Oncol* 2002; 29:31.
7. Boonstra J, Rijken P, Humbel B, et al. The epidermal growth factor. *Cell Biol Int* 1995;19:413.
8. Hidalgo M, Siu LL, Nemunaitis J, et al. Phase I and pharmacologic study of OSI-774, an epidermal growth factor receptor tyrosine kinase inhibitor, in patients with advanced solid malignancies. *J Clin Oncol* 2001;19:3267.
9. Tobita K, Kijima H, Dowaki S, et al. Epidermal growth factor receptor expression in human pancreatic cancer: Significance for liver metastasis. *Int J Mol Med* 2003;11:305.
10. Bruns CJ, Solorzano CC, Harbison MT, et al. Blockade of the epidermal growth factor receptor signaling by a novel tyrosine kinase inhibitor leads to apoptosis of endothelial cells and therapy of human pancreatic carcinoma. *Cancer Res* 2000;60:2926.
11. Solorzano CC, Baker CH, Tsan R, et al. Optimization for the blockade of epidermal growth factor receptor signaling for therapy of human pancreatic carcinoma. *Clin Cancer Res* 2001;7: 2563.
12. Baker CH, Kedar D, McCarty MF, et al. Blockade of epidermal growth factor receptor signaling on tumor cells and tumor-associated endothelial cells for therapy of human carcinomas. *Am J Pathol* 2002;161:929.
13. Durkin AJ, Bloomston PM, Rosemurgy AS, et al. Defining the role of the epidermal growth factor receptor in pancreatic cancer grown *in vitro*. *Am J Surg* 2003;186:431.
14. Zervos EE, Norman JG, Gower WR, et al. Matrix metalloproteinase inhibition attenuates human pancreatic cancer growth *in vitro* and decreases mortality and tumorigenesis *in vivo*. *J Surg Res* 1997;69:367.
15. Denham DW, Franz MG, Denham W, et al. Directed anti-sense therapy confirms the role of protein kinase C- α in the tumorigenicity of pancreatic cancer. *Surgery* 1998;124: 218; discussion 223.
16. Zervos EE, Shafii AE, Rosemurgy AS. Matrix metalloproteinase (MMP) inhibition selectively decreases type II MMP activity in a murine model of pancreatic cancer. *J Surg Res* 1999;81:65.
17. Zervos EE, Franz MG, Salhab KF, et al. Matrix metalloproteinase inhibition improves survival in an orthotopic model of human pancreatic cancer. *J Gastrointest Surg* 2000;4:614.
18. Haq M, Shafii A, Zervos EE, Rosemurgy AS. Addition of matrix metalloproteinase inhibition to conventional cytotoxic therapy reduces tumor implantation and prolongs survival in a murine model of human pancreatic cancer. *Cancer Res* 2000;60:3207.
19. Allred DC, Harvey JM, Berardo M, et al. Prognostic and predictive factors in breast cancer by immunohistochemical analysis. *Mod Pathol* 1998;11:155.
20. Mendelsohn J, Baselga J. The EGF receptor family as targets for cancer therapy. *Oncogene* 2000;19:6550.
21. Xiong HQ, Rosenberg A, LoBuglio A, et al. Cetuximab, a monoclonal antibody targeting the epidermal growth factor receptor, in combination with gemcitabine for advanced pancreatic cancer: a multicenter phase II Trial. *J Clin Oncol* 2004;22:2610.
22. Diaz-Rubio E. New chemotherapeutic advances in pancreatic, colorectal, and gastric cancers. *Oncologist* 2004;9:282.
23. Kim T. Technology evaluation: Matuzumab, Merck KGaA. *Curr Opin Mol Ther* 2004;6:96.
24. Jiang K, Delarue FL, Sefti SM. EGFR, ErbB2 and Ras but not Src suppress RhoB expression while ectopic expression of RhoB antagonizes oncogene-mediated transformation. *Oncogene* 2004;23: 1136.
25. Parikh AA, Liu WB, Fan F, et al. Expression and regulation of the novel vascular endothelial growth factor receptor neuropilin-1 by epidermal growth factor in human pancreatic carcinoma. *Cancer* 2003;98:720.
26. Scwabas GM, Fujioka S, Schmidt C, et al. Restoring apoptosis in pancreatic cancer cells by targeting the nuclear factor-kappaB signaling pathway with the anti-epidermal growth factor antibody IMC-C225. *J Gastrointest Surg* 2003;7:37; discussion 43.
27. Lee LT, Huang YT, Hwang JJ, et al. Blockade of the epidermal growth factor receptor tyrosine kinase activity by quercetin and luteolin leads to growth inhibition and apoptosis of pancreatic tumor cells. *Anticancer Res* 2002;22:1615.

Featured Article

Intravenous RNA Interference Gene Therapy Targeting the Human Epidermal Growth Factor Receptor Prolongs Survival in Intracranial Brain Cancer

Yun Zhang,¹ Yu-feng Zhang,¹ Joshua Bryant,²
Andrew Charles,² Ruben J. Boado,^{1,3} and
William M. Pardridge¹

Departments of ¹Medicine and ²Neurology, University of California
Los Angeles, Los Angeles, California and ³Armagen Technologies,
Inc., Santa Monica, California

ABSTRACT

Purpose: The human epidermal growth factor receptor (EGFR) plays an oncogenic role in solid cancer, including brain cancer. The present study was designed to prolong survival in mice with intracranial human brain cancer with the weekly i.v. injection of nonviral gene therapy causing RNA interference (RNAi) of EGFR gene expression.

Experimental Design: Human U87 gliomas were implanted in the brain of adult scid mice, and weekly i.v. gene therapy was started at day 5 after implantation of 500,000 cells. An expression plasmid encoding a short hairpin RNA directed at nucleotides 2529–2557 within the human EGFR mRNA was encapsulated in pegylated immunoliposomes. The pegylated immunoliposome was targeted to brain cancer with 2 receptor-specific monoclonal antibodies (MAb), the murine 83–14 MAb to the human insulin receptor and the rat 8D3 MAb to the mouse transferrin receptor.

Results: In cultured glioma cells, the delivery of the RNAi expression plasmid resulted in a 95% suppression of EGFR function, based on measurement of thymidine incorporation or intracellular calcium signaling. Weekly i.v. RNAi gene therapy caused reduced tumor expression of immunoreactive EGFR and an 88% increase in survival time of mice with advanced intracranial brain cancer.

Conclusions: Weekly i.v. nonviral RNAi gene therapy directed against the human EGFR is a new therapeutic approach to silencing oncogenic genes in solid cancers. This is enabled with a nonviral gene transfer technology that delivers liposome-encapsulated plasmid DNA across cellular barriers with receptor-specific targeting ligands.

INTRODUCTION

The human epidermal growth factor receptor (EGFR) plays an oncogenic role in 90% of primary brain cancers such as glioblastoma multiforme (1). In addition, the EGFR plays an oncogenic role in 70% of solid cancers that originate outside the brain (2). Because many solid cancers of peripheral organs metastasize to the brain, the EGFR plays a tumorigenic role in both primary brain cancer, as well as metastatic cancer to the brain. The development of brain cancer therapeutics, which knock-down the function of the EGFR, is made difficult by the presence of the blood-brain barrier (BBB). The BBB is formed by blood vessels that originate from normal brain, which perfuse the primary or metastatic cancer in brain. In the early and intermediate stages of brain cancer when therapeutic intervention is desirable, the capillaries perfusing the brain cancer have restrictive permeability properties (3), similar to capillaries in normal brain, which form the BBB (4). The problems presented by the BBB in the development of brain cancer therapeutics are illustrated in the case of Herceptin, a humanized monoclonal antibody to the HER2 receptor, which is a member of the *EGFR* gene family. Although Herceptin inhibits growth of HER2-positive cancer in the breast, this therapeutic is not effective against breast cancer that has metastasized to the brain (5). Large-molecule therapeutics, such as monoclonal antibodies or gene therapies, cannot cross the BBB.

Gene therapy of brain cancer offers the promise of specifically knocking down the expression of oncogenic genes such as *EGFR*. However, gene therapy is limited by the delivery problem, which is particularly difficult in brain because of the presence of the BBB. To circumvent the BBB, attempts have been made to deliver therapeutics to brain cancer by craniotomy. However, this approach is not effective, because there is limited diffusion of the therapeutic gene within the tumor from the *trans*-cranial injection site (6). Therapeutics can be delivered to all of the cells in brain cancer via the *trans*-vascular route across the BBB (4). The *trans*-vascular delivery of nonviral genes to brain is possible with a gene transfer technology that uses pegylated immunoliposomes (PILs; Ref. 7). With this approach, the nonviral plasmid DNA is encapsulated in the interior of an 85-nm anionic liposome, and the surface of the liposome is conjugated with several thousand strands of polyethylene glycol (PEG). This “PEGylation” process restricts uptake of the liposome by the reticuloendothelial system and enables a prolonged blood residence time (8). The PEGylated liposome is then targeted across biological barriers *in vivo* with receptor-specific peptidomimetic monoclonal antibodies (MAbs) as depicted in Fig. 1A. The application of the PIL nonviral gene transfer technology enabled a 100% increase in survival time of mice with intracranial human brain cancer with weekly i.v. injections of antisense gene therapy directed at the human EGFR (9). A eukaryotic expression plasmid, designated clone 882, which encodes for a 700 nucleotide RNA that is antisense to nucleo-

Received 12/15/03; revised 2/13/04; accepted 2/25/04.

Grant support: Accelerate Brain Cancer Cure, Inc., NIH Grant R01-NS-39961, and NIH Grant R43-CA-109782.

The costs of publication of this article were defrayed in part by the payment of page charges. This article must therefore be hereby marked *advertisement* in accordance with 18 U.S.C. Section 1734 solely to indicate this fact.

Requests for reprints: William M. Pardridge, University of California Los Angeles, Warren Hall 13-164, 900 Veteran Avenue, Los Angeles, CA 90024. Phone: (310) 825-8858; Fax: (310) 206-5163; E-mail: wpardridge@mednet.ucla.edu.

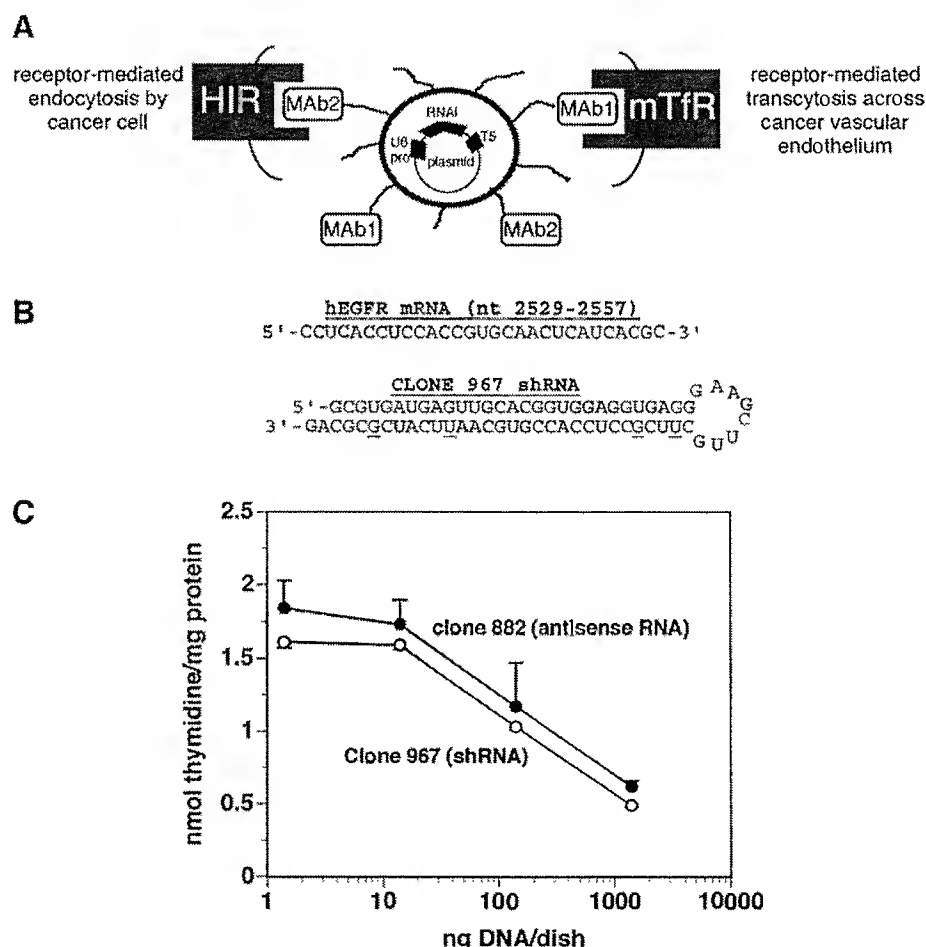


Fig. 1 Delivery of epidermal growth factor receptor RNA interference genes with pegylated immunoliposomes. **A**, model of pegylated immunoliposome (PIL) that is doubly targeted to both the mouse transferrin receptor (*mTfR*) with the 8D3 monoclonal antibody (*MAb1*) and to the human insulin receptor (*HIR*) with the 83-14 monoclonal antibody (*MAb2*). Encapsulated in the interior of the PIL is the plasmid DNA encoding the short hairpin RNA (*shRNA*), which produces the RNA interference (*RNAi*). The gene encoding the *shRNA* is driven by the U6 promoter (*pro*) and is followed on the 3'-end with the T5 termination sequence for the U6 RNA polymerase. **B**, nucleotide sequence of the human epidermal growth factor receptor (*hEGFR*) sequence between nucleotides 2529 and 2557 is shown on top. The sequence and secondary structure of the *shRNA* produced by clone 967 is shown on the bottom. The antisense strand is 5' to the 8 nucleotide loop, and the sense strand is 3' to the loop. The sense strand contains 4 G/U mismatches to reduce the *T_m* of hybridization of the stem loop structure; the sequence of the antisense strand is 100% complementary to the target mRNA sequence. **C**, human U87 glioma cells were incubated with [³H]thymidine for a 48 h period that follows a 5-day period of incubation of the cells with HIRMAb-targeted PILs carrying either clone 967 or 882 plasmid DNA. A dose of 1.4, 14, 140, or 1400 ng plasmid DNA per dish was used in each experiment. Data are mean (*n* = 3 dishes); bars, \pm SE.

tides 2317–3006 of the human EGFR (10), was encapsulated in PILs that were doubly targeted to brain cancer *in vivo* with 2 MAbs of different receptor specificities (9). One MAb, the rat 8D3 MAb to the mouse transferrin receptor (TfR), enabled transport of the PIL across the mouse BBB forming the microvasculature of the intracranial cancer. A second MAb targeted the human insulin receptor (HIR) that was expressed on the human brain cancer plasma membrane (Fig. 1A). The targeting MAbs act as molecular Trojan horses to ferry the PIL across membrane barriers, and these MAbs are species specific (7). The 8D3 to the mouse TfR enables transport across the first barrier, the mouse BBB, but does not mediate transport of the PIL across the second barrier, the human brain cancer cell membrane. This is accomplished with the HIRMAb, which does

not react with the mouse vascular endothelial insulin receptor. The doubly conjugated PIL is designated HIRMAb/TfRMAb-PIL (Fig. 1A). To augment the potency of the clone 882 expression plasmid, this vector contained the oriP and Epstein-Barr nuclear antigen (EBNA)-1 elements (10), which allow for a single round of replication of the expression plasmid with each division of the cancer cell (11). The inclusion of the oriP/EBNA-1 elements within the expression plasmid enables a 10-fold increase in the level of gene expression in human U87 glioma cells (12). However, the *EBNA-1* gene encodes a tumorigenic *trans*-acting factor (13), and this formulation may not be desirable in human gene therapy. It is possible that the EBNA-1 element would not be required if a more potent form of antisense gene therapy were used.

RNA interference (RNAi) is a new form of antisense gene therapy wherein an expression plasmid encodes for a short hairpin RNA (shRNA) that is composed of a stem-loop structure (14). This shRNA is processed in the cell to an RNA duplex with a 3'-overhang, and this short RNA duplex mediates RNAi or post-transcriptional gene silencing. Although RNAi-based gene therapy offers promise for the treatment of cancer, the limiting factor is delivery. Therefore, the present studies were designed to test the therapeutic efficacy of i.v. RNAi-based gene therapy directed at the human EGFR in mice with brain cancer. A new expression plasmid was designed, which lacked the oriP/EBNA-1 elements and which encoded for an shRNA directed at a specific sequence in the human EGFR mRNA, and this plasmid was incorporated in HIRMAb/TfRMAb-PILs. These PILs were administered i.v. on a weekly schedule to mice with intracranial human brain cancer.

MATERIALS AND METHODS

Materials. 1-Palmitoyl-2-oleoyl-*sn*-glycerol-3-phosphocholine and dimethyldioctadecylammonium bromide were purchased from Avanti-Polar Lipids, Inc. (Alabaster, AL). Distearoylphosphatidylethanolamine-PEG²⁰⁰⁰ was obtained from Shearwater Polymers (Huntsville, AL), where PEG²⁰⁰⁰ is 2000 Dalton polyethyleneglycol. Distearoylphosphatidylethanolamine-PEG²⁰⁰⁰-maleimide was custom synthesized by Shearwater Polymers. [α -³²P]dCTP (3000 Ci/mmol) was from Perkin-Elmer (Boston, MA), and *N*-succinimidyl[2,3-³H]propionate (101 Ci/mmol) and protein G Sepharose CL-4B were purchased from Amersham-Pharmacia Biotech (Arlington Heights, IL). The 2-iminothiolane (Traut's reagent) and bicinchoninic acid protein assay reagents were obtained from Pierce Chemical Co. (Rockford, IL). The anti-TfRMAb used in this study is the 8D3 rat MAb to the mouse TfR (15). The 8D3 MAb is specific for the mouse TfR and is not active in human cells. The anti-insulin receptor MAb used for gene targeting to human cells is the murine 83-14 MAb to the human insulin receptor (HIR; Ref. 16). The TfRMAb and HIRMAb were individually purified with protein G affinity chromatography from hybridoma generated ascites. Custom oligodeoxynucleotides (ODNs) were obtained from Biosource (Camarillo, CA). The nick translation system and the *Escheria coli* DH5 α competent cells were purchased from Invitrogen (San Diego, CA). All of the restriction endonucleases were obtained from New England Biolabs (Boston, MA). Horse serum, rabbit serum, donkey serum, mouse IgG1 isotype, rat IgG, and glycerol-gelatin were from Sigma-Aldrich Chemical Co. (St. Louis, MO). The biotinylated horse antimouse IgG, biotinylated rabbit antirat IgG, Vectastain ABC kit, 3-amino-9-ethylcarbazole substrate kit, and Vectashield mounting medium were purchased from Vector Laboratories (Burlingame, CA); 488 Alexa fluor donkey antimouse IgG and 594 Alexa fluor donkey antirat IgG were obtained from Molecular Probes (Eugene, OR). OCT compound (Tissue-Tek) was purchased from Sakura FineTek (Torrance, CA).

Construction of Expression Plasmids. ODN duplexes corresponding to the various EGFR shRNAs were designed as described by Paddison *et al.* (17), and shown in Table 1. The shRNA sequence intentionally included nucleotide mismatches in the sense strand (Fig. 1B) to reduce the formation of DNA

hairpins during cloning. Because the antisense strand remains unaltered, these G-U substitutions do not interfere with the RNAi effect (18). Forward ODNs contain a U6 polymerase stop signal (T₆; Table 1). Reverse ODNs contain 4-nucleotide overhangs specific for the *Eco*RI and *Apa*I restriction sites at 5'- and 3'-end, respectively (Table 1), to direct subcloning into the cohesive ends of the expression plasmid (19). The empty expression plasmid is designated clone 959 (Table 2). Complementary ODNs were heat denatured (4 min at 94°C) and annealed at 65°C for 16 h in 10 mM sodium phosphate (pH = 7.4), 150 mM sodium chloride, and 1 mM EDTA. Double-stranded ODNs were ligated into the expression plasmid at *Eco*RI and *Apa*I sites. *E. coli* DH5 α competent cells were transformed, and clones with the correct RNAi inserts were confirmed by DNA sequencing using the T3 primer and restriction endonuclease mapping with *Nae*I.

A total of 6 anti-EGFR shRNA encoding expression plasmids were produced and designated clones 962-964 and 966-968 (Tables 1-2). The sequence of the antisense strand of each of the 6 shRNAs matches 100% with the target sequence of the human EGFR (accession no. X00588). The EGFR knockdown potency of these 6 shRNA encoding expression plasmids was compared with the EGFR knockdown effect of clone 882, which is a eukaryotic expression plasmid described previously (10). Clone 882 is derived from pCEP4, is driven by the SV40 promoter, contains EBNA-1/oriP elements, and encodes for a 700 nucleotide antisense RNA complementary to nucleotides 2317-3006 of the human EGFR (10). The RNAi effect on the human EGFR was screened by measuring the rate of [³H]thymidine incorporation into human U87 glioma cells in tissue culture.

Thymidine Incorporation in U87 Glioma Cells. U87 human glioma cells were grown in six-well cluster dishes with MEM containing 10% fetal bovine serum. After the cells reached 50-60% confluence, the growth medium was replaced with 1.5 ml of serum-free MEM containing 1 μ g of each plasmid DNA (clone 959, 962-964, 966-968, or 882) and 10 μ l (20 μ g) of Lipofectamine and incubated for 4 h at 37°C. The medium was replaced with MEM with 10% fetal bovine serum and incubated for 24 h. A final concentration of 2 μ Ci/ml of [³H]thymidine and 10 μ M of unlabeled thymidine were added to each dish, and dishes were incubated at 37°C for 48 h. The cells were harvested for measurement of [³H]thymidine incorporation as described previously (10).

The transfection of the U87 cells with Lipofectamine demonstrated that clone 967 was the most potent clone causing RNAi of EGFR expression. A dose response study with clone 967 was performed, in parallel with a dose response study for clone 882, which encodes for the 700 nucleotide EGFR antisense RNA (10). U87 cells were grown on 35-mm collagen-treated dishes. After the cells reached 50-60% confluence, the medium was aspirated, and 2 ml of fresh MEM with 10% fetal bovine serum and HIRMAb-PILs encapsulated with clone 967 or clone 882 at a dose of 1.4, 0.14, 0.014, or 0.0014 μ g DNA/dish were added. The cells were incubated for 5 days at 37°C. During this period, 2 ml of fresh medium was added after 3 days of incubation. At 5 days, the medium was aspirated, and 2 ml of fresh growth medium containing 2 μ Ci/ml of [³H]thymidine and 10 μ M of unlabeled thymidine were added to each

Table 1 Design of shRNA^a to target EGFR mRNA: list of ODNs used for the construction of expression plasmids

Nucleotide overhangs to the *EcoRI* and *ApaI* restriction sites at 5'- and 3'-end of reverse ODNs are underlined. EGFR mRNA nucleotide sequences are taken from accession no. X00588.

Plasmid number	EGFR mRNA (nt)	ODN sequence
962	187–219	Forward: GCTGCCCCGGCCGTCCCGAGGGTCGCATGAAGCTTGATGCGACTCTTCGGGACGGTCGGGGTAGCGCTTTTTT Reverse: <u>AATTAAAAAAGCGCTACCCCGACCGTCCCGAAGAGTCGCATCAAGCTTCATGCGACCCCTCCGGGACGGCCGG</u> GGCAGCGGCC
963	2087–2119	Forward: GATCTTAGGCCCATTCGTTGGACAGCCTTGAAGCTTGAGGGTTGTCGACGAATGGGCCTAAGATTCCTTTTTT Reverse: <u>AATTAAAAAAGGAATCTTAGGCCCATTCGTCGGACAACCCCTCAAGCTTCAAGGCTGTCCAACGAATGGGCCT</u> AAGATCGGCC
964	3683–3715	Forward: GTCCTGCTGGTAGTCAGGGTTGTCCAGGCGAAGCTTGGTCTGGATAATCCTGACTATCAGCAGGACTTTTTTTTT Reverse: <u>AATTAAAAAAGTCTGCTGATAGTCAGGATTATCCAGACCAAGCTTCGCCTGGACAACCTGACTACCAGC</u> AGGACGGCC
966	2346–2374	Forward: GTCCCTTATACACCGTGCCGAACGCACCGGAAGCTTGCGGTGCGTTCGGCGCGGTGTGTGAGGGATTCTTTTTT Reverse: <u>AATTAAAAAAGAATCCCTCACACACCGCGCCGAACGCACCGCAAGCTTCGGGTGCGTTCGGCACGGTGTATAA</u> GGGACGGCC
967	2529–2557	Forward: GCGTGATGAGTTGCACGGTGGAGGTGAGGGAAGCTTGCTTCGCCTCCACCGTGCAATTCATCGCGCAGTTTTTTT Reverse: <u>AATTAAAAAAGTGCATGAATTGCACGGTGGAGGCGAAGCAAGCTTCCTCACCTCCACCGTGCAACTCAT</u> CACGCGGCC
968	2937–2965	Forward: GGATGGAGGAGATCTCGCTGGCAGGGATTGAAGCTTGAGTCTCTGCGCGGAGATCTCCTCCGTCCTGTTTTTT Reverse: <u>AATTAAAAACAGGACGGAGAGATCTCGCGGCAGAGACTCAAGCTTCAATCCCTGCCAGCGAGATCTCCT</u> CCATCCGGCC

^a shRNA, short hairpin RNA; EGFR, epidermal growth factor receptor; ODN, oligodeoxynucleotide; nt, nucleotide.

dish, followed by a 48-h incubation at 37°C. At the end of the incubation, [³H]thymidine incorporation was measured and expressed as nmol thymidine incorporated/mg cell protein, as described previously (10).

EGFR Western Blotting. Human U87 cells were grown in 35-mm dishes to 80% confluency and then exposed for 4 h to serum-free medium containing 1.5 µg/dish clone 967, 962, 952, or 882 in Lipofectamine, as described previously (10). Clones 962 and 967 produce an anti-EGFR shRNA clone (Tables 1–2), clone 882 produces a 700 nucleotide RNA antisense to the human EGFR mRNA (10), and clone 952 produces an shRNA directed against the luciferase mRNA, as described previously (19). After the initial 4-h incubation, the medium was replaced with fresh medium containing 10% fetal bovine serum, and the cells were harvested 48 h later for electrophoresis through a reducing 7.5% SDS-PAGE and blotting to nitrocellulose. The primary antibody was a 1:1000 dilution of the rabbit polyclonal antibody (#2232) to the human EGFR from Cell Signaling Technology (Beverly, MA). The secondary antibody was a conjugate of peroxidase and a goat-antirabbit antibody from Sigma (A0545), and the immune reaction was determined with the enhanced chemiluminescence method as described previously (10). The X-ray film was scanned into Adobe PhotoShop and intensity of the band corresponding to the 170 kDa immunoreactive EGFR was quantified with NIH Image software.

Synthesis of PILs. Clone 967 or 882 plasmid DNA was encapsulated in PILs as described previously (8, 10, 20). The liposome was 85–100 nm in diameter, and the surface of the liposome was conjugated with several thousand strands of 2000 Da PEG. The tips of about 1–2% of the PEG strands were conjugated with 83–14 HIRMAb and the 8D3 TIRMAb, as described previously (9). Any plasmid DNA not encapsulated in the interior of the liposome was quantitatively removed by exhaustive nuclease treatment (8). In a typical synthesis, 30–40% of the initial plasmid DNA (200 µg) was encapsulated

within 20 µmol of lipid, and each liposome had a range of 43–87 MAb molecules conjugated to the PEG strands (9).

Calcium Signaling. U87 cells were grown in 35-mm plastic flasks and passaged onto 18-mm diameter glass coverslips in 12-well plates. Growth medium was composed of DMEM-F12 supplemented with 5% fetal bovine serum, 5% horse serum, penicillin, and streptomycin. Cells were grown at 37° in a humidified incubator with 5% CO₂. At 1–2 days after passage, cells were exposed to HIRMAb-PILs carrying clone 967 plasmid DNA by addition of the PILs directly to the wells

Table 2 shRNA^a target site within human EGFR mRNA and biological activity in U87 cells

Human U87 glioma cells were incubated with 1 µg plasmid DNA and 20 µg Lipofectamine in serum-free medium for 4 h. The medium was then replaced, and 24 h later [³H]thymidine (2 µCi/ml) and 10 µM unlabeled thymidine were added, and the cells were incubated for a 48-h period before measurement of thymidine incorporation. Data are mean ± SE (*n* = 3 dishes).

Plasmid number	RNA type	EGFR mRNA sequence	Thymidine incorporation (% inhibition) ^b
959	None	None	0
962	shRNA	187–219	0
963	shRNA	2087–2119	0
966	shRNA	2346–2374	59 ± 1
967	shRNA	2529–2557	97 ± 3
968	shRNA	2937–2965	72 ± 3
964	shRNA	3683–3715	59 ± 3
882	Antisense	2317–3006	100

^a shRNA, short hairpin RNA; EGFR, epidermal growth factor receptor.

^b % inhibition of thymidine incorporation = [(A – B)/(A – C)] × 100, where A = thymidine incorporation with clone 959 (the empty expression plasmid), B = thymidine incorporation with clone 962, 963, 964, 966, 967, or 968, and C = thymidine incorporation with clone 882.

without medium exchange. Cells were maintained in the same medium (with or without PILs) for 12–48 h before experimentation. Epidermal growth factor (EGF) has been shown to evoke intracellular calcium signaling in brain tumor cells (21), and a similar response in human U87 glioma cells was found in these studies. Changes in $[Ca^{2+}]_i$ were measured using a video imaging system as described previously (22). Cells were incubated at room temperature for 30 min–1 h in HBSS containing 2.5 μ M fluo-4-AM (Molecular Probes). Cells were then washed and maintained in fresh medium for at least 30 min to allow complete de-esterification of dye. Cells were then placed in an open slide flow-chamber on the stage of a Nikon inverted microscope. Changes in $[Ca^{2+}]_i$ in fields of cells (typically 60–80 cells/field) were measured with 488-nm excitation via a Nikon $\times 20$ epifluorescence objective. Fluorescence at 510 nm was recorded with a silicon-intensified tube camera (Hamamatsu) and digitized at a resolution of 640×480 pixels using an Axon Image Lightning board and Image WorkBench software. Spontaneous activity was recorded for 60–120 min, after which EGF (200 ng/ml in HBSS) was applied by bath perfusion. The change in fluorescence of fluo-4 for individual cells in the field was displayed as a continuous record showing the time course of change in fluorescence for regions of interest drawn for each individual cell. A response to EGF, ATP, or bradykinin was defined as an increase in fluo-4 fluorescence of at least 20% above baseline during 120 s of EGF exposure.

In Vivo Brain Cancer Model. All of the animal procedures were approved by the University of California Los Angeles Animal Research Committee. Female severe combined immunodeficient (scid) mice weighing 19–21 g were purchased from the Jackson Laboratory (Bar Harbor, ME). A burr hole was drilled 2.5 mm to the right of midline and 1 mm anterior to bregma. U87 glioma cells were suspended in serum-free MEM containing 1.2% methylcellulose. Five μ l of cell suspension (5×10^5 cells) were injected into the right caudate-putamen nucleus at a depth of 3.5 mm over 2 min, using a 10- μ l Hamilton syringe with fixed needle. The animals were treated i.v. once a week starting at day 5 after implantation. By 5 days after the implantation of 500,000 U87 cells, the tumor is large and fills the entire volume of the striatum in brain (23). Weekly i.v. gene therapy was administered at 5, 12, 19, and 26 days after implantation. Mice were treated with either saline or 5 μ g/mouse of clone 967 DNA encapsulated in the HIRMAb/TfRMAb-PILs.

Confocal Microscopy and Immunocytochemistry. Brains were removed immediately after sacrifice and cut into coronal slabs from the center of tumor. Slabs were embedded in OCT medium and frozen in dry ice powder. Frozen sections (20 μ m) of mouse brain were cut on a Mikron HM505E cryostat. Sections were fixed in cold 100% methanol for 20 min at -20°C . For confocal microscopy, nonspecific binding of proteins was blocked with 10% donkey serum-PBS for 30 min. The sections were incubated in primary antibody overnight at 4°C . The primary antibodies were the rat 8D3 MAb to the mouse TfR (10 μ g/ml) and the mouse 528 MAb against the human EGFR (10 μ g/ml). After a PBS wash, a rhodamine-conjugated donkey antirat IgG secondary antibody, 5 μ g/ml, was added for 30 min at room temperature. The slides were then washed and incubated with fluorescein-conjugated goat antimouse IgG at 5 μ g/ml for

30 min at room temperature. The sections were mounted on slides, and viewed with a $\times 4X$ objective and a Zeiss LSM 5 PASCAL confocal microscope with dual argon and helium/neon lasers. The sample was scanned in multitrack mode to avoid leakage of the fluorescein signal into the rhodamine channel. Sections were scanned at intervals of 0.8 μ m and reconstructed with Zeiss LSM software. Control experiments used either a rat IgG (Sigma) or a mouse IgG1 (Sigma) as primary antibodies in lieu of the rat antimouse TfR or the mouse antihuman EGFR antibody, respectively.

Immunocytochemistry was performed by the avidin-biotin complex immunoperoxidase method (Vector Laboratories). To stain the human EGFR, the mouse 528 MAb antihuman EGFR was used as the primary antibody (24); to stain the mouse TfR, the rat 8D3 MAb antimouse TfR was used as the primary antibody (9). Endogenous peroxidase was blocked with 0.3% H_2O_2 in 0.3% horse serum-PBS for 30 min; nonspecific binding of proteins was blocked with 3% horse or rabbit serum in PBS for 30 min. For mouse TfR staining using rat 8D3 MAb, rabbit serum was used in the blocking steps. Sections were then incubated in 10 μ g/ml of primary antibody overnight at 4°C . Identical concentrations of isotype control antibody were also used as primary antibody. Mouse IgG1 was used as the isotype antibody for 528 MAb, and rat IgG was used as the isotype control antibody for 8D3 MAb. After incubation and wash in PBS, sections were incubated in either biotinylated horse antimouse IgG (for 528 MAb) or biotinylated rabbit antirat IgG (for 8D3 MAb) for 30 min, before color development with 3-amino-9-ethylcarbazole. Slides were not counterstained. The sections immunostained with the mouse vascular specific marker, the TfRMAb, were quantified with light microscopy and an optical grid and expressed as capillaries per 0.1 mm^2 of brain tissue.

RESULTS

Design of shRNA Encoding Plasmid. Forward and reverse synthetic ODNs were designed to produce shRNAs directed at three broadly spaced regions of the human EGFR mRNA at nucleotides 187–219 (clone 962), 2087–2119 (clone 963), and 3683–3715 (clone 964), and the ODN sequences are given in Table 1. The biological activity of the EGFR RNAi plasmids was tested by measuring the inhibition of $[^3\text{H}]$ thymidine incorporation in U87 human glioma cells (Table 2). Clones 962–963 caused no knockdown of EGFR action, and the effect of clone 964 was intermediate (Table 2). Therefore, a second series of ODNs were designed to produce shRNAs directed at three different regions within nucleotides 2300–3000 of the human EGFR mRNA, including 2346–2374 (clone 966), 2529–2557 (clone 967), and 2937–2965 (clone 968) as shown in Table 1. Whereas the knockdown of EGFR function was intermediate with clones 966 and 968, clone 967 produced a level of inhibition of $[^3\text{H}]$ thymidine incorporation comparable with clone 882 (Table 2). The sequence and secondary structure of the shRNA produced by clone 967 is shown in Fig. 1B.

The anti-EGFR shRNA encoding plasmids were initially delivered to U87 human glioma cells with Lipofectamine (Table 2). Clone 967 or 882 plasmid DNA were then encapsulated in HIRMAb-targeted PILs and added to U87 cells without Lipofectamine at various doses of plasmid DNA ranging from 1.4 to

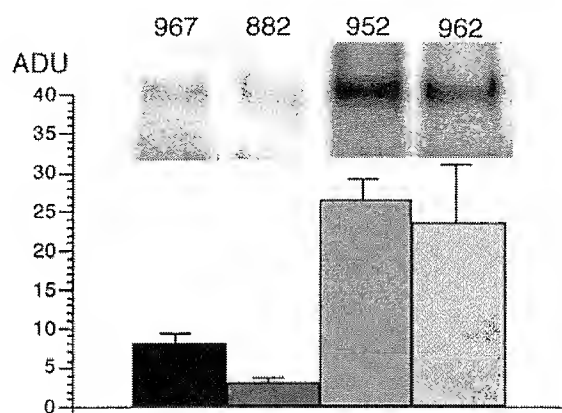


Fig. 2 Epidermal growth factor receptor Western blotting. U87 human glioma cells were exposed to clone 967, clone 882, clone 952, or clone 962 plasmid DNA for 48 h and harvested for epidermal growth factor receptor Western blotting. Films were scanned and quantified with NIH Image software; arbitrary densitometric units (ADU) were computed for each treatment group. A representative scan is shown at the top of each mean ($n = 3-4$ dishes); bars, \pm SE.

1400 ng/dish. Either plasmid DNA was equally active in suppressing thymidine incorporation with an ED_{50} of ~ 100 ng/dish (Fig. 1C).

Western Blotting. The EGFR Western blots are shown in Fig. 2, as are the results of the scanning densitometry of the intensity of the 170 kDa EGFR band (Fig. 2, top). There is no significant difference in the level of the immunoreactive EGFR in the cells exposed to either clone 952, which produces an shRNA directed against luciferase (19), or clone 962, which produces an shRNA against an inactive site of the EGFR mRNA (Table 2). However, exposure of the cells to either clone 967 or clone 882 caused a 68% and 88% inhibition of the expression of the immunoreactive EGFR, respectively (Fig. 2).

Calcium Signaling in U87 Glioma Cells in Tissue Culture. To confirm the inhibition of functional EGFR expression by PIL-mediated RNAi in cell culture, we examined Ca^{2+} signaling in U87 cells in response to EGF using fluorescence video microscopy. The majority of U87 cells respond to EGF (200 ng/ml) with an increase in $[Ca^{2+}]_i$ that begins 10–30 s after exposure to EGF and continues for 60–300 s (Table 3; Fig. 3A). Treatment of U87 cells with HIRMAb-PILs containing 0.125 μ g clone 967 plasmid DNA per 18 mm coverslip resulted in a significant reduction in the number of cells responding to EGF, whereas treatment with 0.25–1.5 μ g DNA of clone 967 abolished the Ca^{2+} response to EGF in nearly all of the cells (Table 3; Fig. 3B). The inhibition of the response to EGF was observed at 12 and 24 h after exposure to the PILs, whereas the Ca^{2+} signaling response was largely restored at 48 h after PIL exposure (Table 3). To determine whether the PILs or shRNA encoding plasmid DNA had any nonspecific effects on Ca^{2+} signaling, we examined the response of the cells to ATP and bradykinin. The percentage of cells responding to ATP (1 μ M) and bradykinin (100 nM) were not significantly different for controls *versus* cells exposed to HIRMAb-targeted PILs encapsulated with clone 967 plasmid DNA (1.5 μ g) for 24 h (Table 3). The amplitude and duration of the Ca^{2+} responses were also

similar, indicating that the treatment did not have a nonspecific effect on Ca^{2+} signaling evoked by other ligands.

Intravenous Anti-EGFR Gene Therapy of Intracranial Brain Cancer. Human U87 glioma cells were implanted in the caudate-putamen nucleus of adult acid mice, which causes death at 14–20 days secondary to the growth of large intracranial tumors. Starting on day 5 after implantation, mice were treated with weekly i.v. injections of either saline or 5 μ g/mouse of clone 967 plasmid DNA encapsulated in PILs that were doubly targeted with both the 83–14 murine MAb to the HIR and the 8D3 rat MAb to the mouse TfR (Fig. 1A). The saline-treated mice died between 14 and 20 days after implantation with an ED_{50} of 17 days (Fig. 4). The mice treated with i.v. gene therapy died between 31 and 34 days postimplantation with an ED_{50} of 32 days, which represents an 88% increase over the ED_{50} in the saline-treated animals (Fig. 4).

The tumors were examined at autopsy by immunocytochemistry using the rat 8D3 MAb to the mouse TfR, which stains the vessels perfusing the tumor (Fig. 5). Unlike the cancer cells, the cells comprising the tumor vessels are of mouse brain origin and express the murine TfR (9). The tumors from the saline-treated animals were well vascularized and expressed the murine TfR (Fig. 5, A–C). Fig. 5B shows the immunoreactive murine TfR on the vascular endothelium of normal brain and the tumor. A blood vessel originating from normal brain and extending into the tumor is visible (see asterisk, Fig. 5B). The border between the tumor and the normal brain frequently had a low vascular density as shown in Fig. 5B. The vascular density in the tumors of the mice treated with clone 967 encapsulated in the HIRMAb/TfRMAb-PIL was visibly reduced (Fig. 5D), although gene therapy did not cause a visible decrease in vascular density in normal brain as shown in Fig. 5E. The vascular density in the tumor center, the tumor periphery, and the con-

Table 3 Effect of EGFR^a RNAi on intracellular calcium flux in human U87 glioma cells

Signaling molecule	RNAi dose (μ g DNA/dish)	Exposure time (hr)	$[Ca^{++}]_i$ response (% of cells)	Cells counted
EGF (200 ng/ml)	0	–	90 \pm 6	360
	0.125	24	21 \pm 8 ^b	180
	0.25	24	12 \pm 3 ^b	180
	0.5	24	4 \pm 2 ^b	180
	1.0	24	4 \pm 3 ^b	180
	1.5	24	6 \pm 4 ^b	180
EGF (200 ng/ml)	0	–	91 \pm 5	180
	1.5	12	5 \pm 3 ^b	180
	1.5	24	6 \pm 4 ^b	180
	1.5	48	63 \pm 4 ^c	180
ATP (1 μ M)	0	–	67 \pm 8	180
	1.5	24	72 \pm 6	180
BK (100 nM)	0	–	94 \pm 2	180
	1.5	24	94 \pm 3	180

^a EGFR, epidermal growth factor receptor; RNAi, RNA interference; EGF, epidermal growth factor; BK, bradykinin.

^b $P < 0.005$ difference from control, which is the RNAi dose = 0. Mean \pm SE.

^c $P < 0.05$ difference from control, which is the RNAi dose = 0. Mean \pm SE.

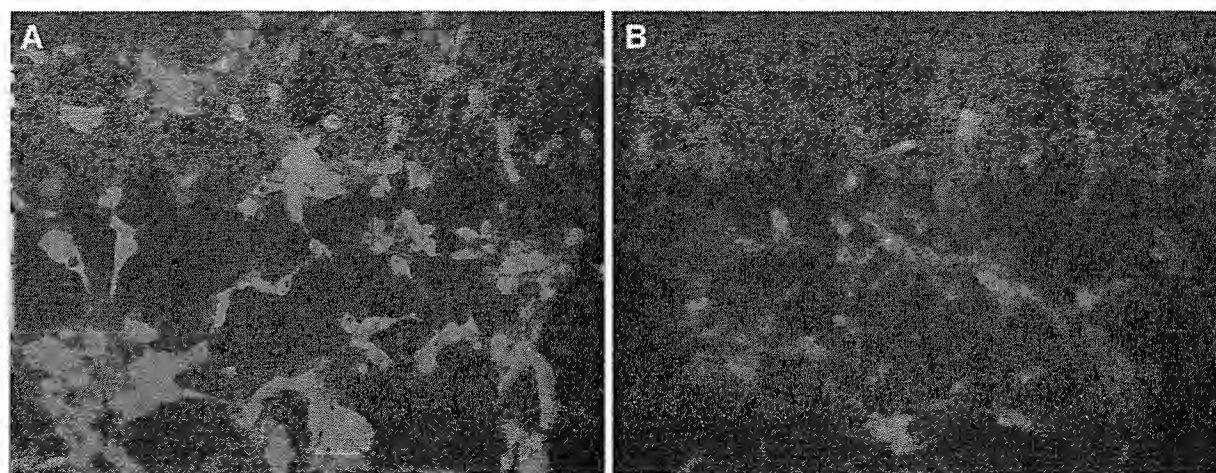


Fig. 3 Knock down of epidermal growth factor receptor-mediated calcium signaling by RNA interference. Maximum Fluo-4 fluorescence in cultured U87 human glioma cells is shown after stimulation with 200 ng/ml human epidermal growth factor. Before measurement of calcium-induced fluorescence, the cells were preincubated for 24 h with either vehicle (A) or HIRMAb-targeted pegylated immunoliposomes carrying clone 967 plasmid DNA at a dose of 0.5 μ g DNA per dish (B).

tralateral normal brain was quantified by light microscopy. Although gene therapy caused no decrease in the vascular density of normal brain, the treatment with clone 967 resulted in an 80% and 72% decrease in vascular density in the tumor center and tumor periphery, respectively, as compared with the saline-treated animals (Table 4).

Confocal Microscopy. The tumor sections were immunostained with both the rat 8D3 MAb to the vascular mouse TfR (red channel) and the murine 528 MAb to the tumor EGFR (green channel) as shown in Fig. 6. There is down-regulation of

the immunoreactive EGFR in the RNAi-treated tumors (Fig. 6, A–C) relative to the saline treated tumors (Fig. 6, D–F).

DISCUSSION

The results of these studies are consistent with the following conclusions. First, it is possible to knock down *EGFR* gene expression with i.v. gene therapy that uses expression plasmids encoding a shRNA directed at nucleotides 2529–2557 of the human *EGFR* mRNA (Table 2). Second, *EGFR* expression knockdown is demonstrated by the inhibition of thymidine incorporation or calcium flux in human U87 glioma cells in tissue culture (Tables 2 and 3; Fig. 3), by the decrease in the expression of immunoreactive EGFR in cell culture (Fig. 2), and by the decrease in brain cancer expression of immunoreactive EGFR *in vivo* (Fig. 6). Third, anti-*EGFR* gene therapy has an antiangiogenic effect and results in a 72–80% decrease in vascular density of the tumor (Fig. 5; Table 4). Fourth, weekly i.v. anti-*EGFR* gene therapy results in an 88% increase in survival time in adult mice with intracranial brain cancer (Fig. 4).

The discovery of RNAi-active target sequences within the human *EGFR* transcript required several iterations (Tables 1 and 2). These findings were consistent with the suggestion of McManus and Sharp (14), that ~1 of 5 target sequences yield therapeutic effects in RNAi. Prior work had shown that *EGFR* gene expression could be inhibited with RNA duplexes delivered to cultured cells with oligofectamine (25). The present studies demonstrate that *EGFR* gene expression can be inhibited with shRNA expression plasmids. The effect of shRNA expression plasmids on *EGFR* gene expression was screened with thymidine incorporation assays (Table 2), because the *EGFR* mediates thymidine incorporation into *EGFR*-dependent cells (26). The thymidine incorporation assays were confirmed by Western blotting, which showed that clones 967 and 882 knock down the *EGFR* (Fig. 2). In contrast, clone 967, which has no effect on thymidine incorporation into U87 cells, also has no effect on the expression of the immunoreactive EGFR (Fig. 2).

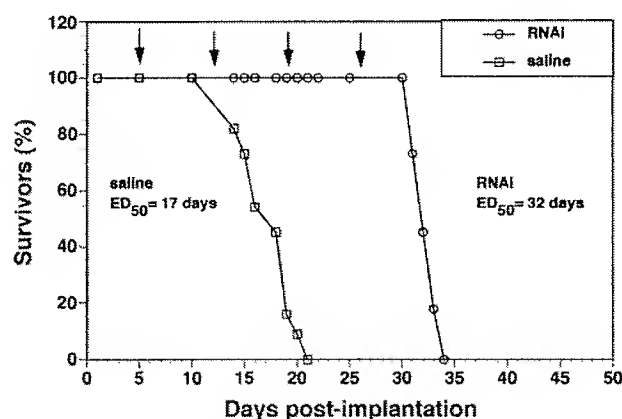


Fig. 4 Survival study. i.v. RNA interference (RNAi) gene therapy directed at the human epidermal growth factor receptor is initiated at 5 days after implantation of 500,000 U87 cells in the caudate putamen nucleus of scid mice, and weekly i.v. gene therapy is repeated at days 12, 19, and 26 (arrows). The control group was treated with saline on the same days. There are 11 mice in each of the two treatment groups. The time at which 50% of the mice were dead (ED_{50}) is 17 days and 32 days in the saline and RNAi groups, respectively. The RNAi gene therapy produces an 88% increase in survival time, which is significant at the $P < 0.005$ level (Fisher's exact test).

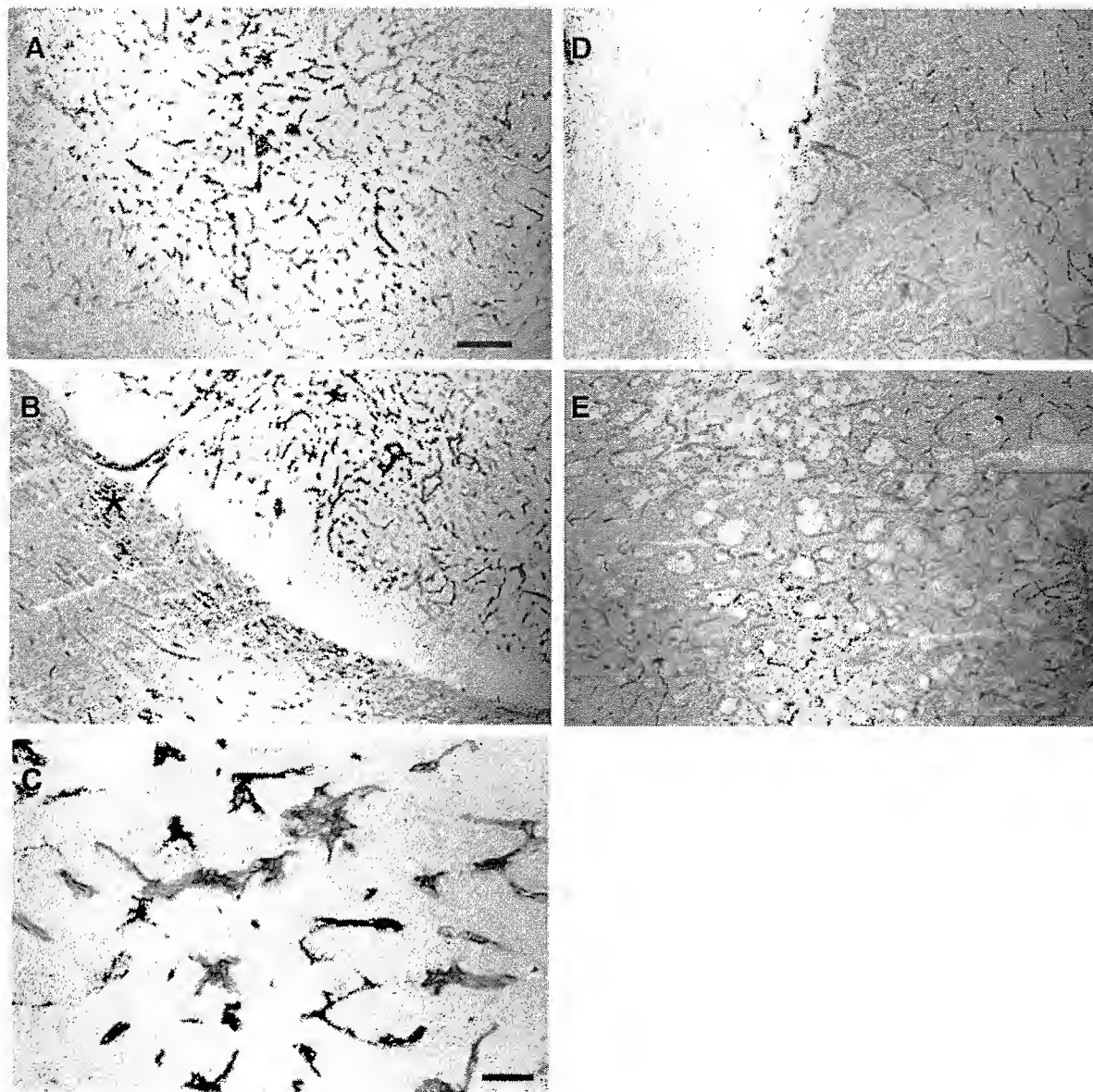


Fig. 5 Immunocytochemistry. Mouse brain autopsy sections are stained with either the rat 8D3 monoclonal antibody to the mouse transferrin receptor (*A–E*) or control rat IgG (not shown). No sections are counterstained. The magnification in panels *A*, *B*, *D*, and *E* is the same, and the magnification bar in *A* is 135 μ m. The magnification bar in *C* is 34 μ m. *A–C* are sections taken from the brain of the saline treated mice, and *D–E* are sections of brain taken from mice treated with the clone 967 gene therapy. *A–C* show the density of the tumor vasculature in the saline treated mice. *B* shows a section containing normal brain at the *bottom* of the panel and tumor at the *top* of the panel; the tumor is vascularized by a vessel originating from normal brain (marked by * in *B*). *D* shows the tumor on the *left* of the panel and normal brain on the *right* of the panel; this section is taken from a mouse treated with RNA interference (RNAi) gene therapy and illustrates the decreased vascular density in the RNAi-treated animals. The vascular density of normal brain is not changed in the RNAi-treated animals as shown in *E*. The control rat IgG primary antibody gave no reaction with mouse brain and the sections are not counterstained or shown.

Similarly, clone 952, which produces an antiluciferase shRNA (19), has no effect on the EGFR (Fig. 2). On the basis of the cell culture work evaluating thymidine incorporation (Table 2) and Western blotting (Fig. 2), clone 967 was chosen for additional evaluation of RNAi-based gene therapy to knock down human *EGFR* gene expression. Clone 967 produces an shRNA directed against nucleotides 2529–2557 (Fig. 1*B*), and this target sequence is within the 700 nucleotide region of the human EGFR

mRNA that is targeted by antisense RNA expressed by clone 882 (10). Clone 967 and clone 882 equally inhibit thymidine incorporation in human U87 cells (Table 2), and this is evidence for the increased potency of RNAi-based forms of antisense gene therapy. The clone 882 plasmid contains the EBNA-1/oriP gene element (10), which enables a 10-fold increase in expression of the *trans*-gene in cultured U87 cells (12). Therefore, the increased potency of the RNAi approach to antisense gene

Table 4 Capillary density in brain tumor and normal brain
Mean \pm SE ($n = 15$ fields analyzed from 3 mice in each of the treatment groups).

Region	Treatment	Capillary density per 0.1 mm ²
Tumor center	Saline	15 \pm 2
	RNAi	3 \pm 0
Tumor periphery	Saline	29 \pm 4
	RNAi	8 \pm 1
Normal brain	Saline	35 \pm 1
	RNAi	33 \pm 1

therapy enabled the elimination of the potentially tumorigenic EBNA-1 element in the expression plasmid.

Clone 967 was delivered to cultured U87 cells with HIRMAb-targeted PILs, and this resulted in a 95% knockdown of EGFR functionality based on measurements of EGFR-induced calcium fluxes (Fig. 3B; Table 3). The RNAi effect of clone 967 was specific to the EGFR, as the PIL delivery of this plasmid to the U87 cells had no effect on ATP- or bradykinin-mediated calcium fluxes in the cells (Table 3). Clone 967 knocked down EGFR function in a dose-dependent mechanism, with respect to inhibition of both calcium flux (Table 3) and

thymidine incorporation (Fig. 1C) with an ED₅₀ of ~ 100 ng plasmid DNA/dish.

Suppression of the EGFR by clone 967 encapsulated in the HIRMAb/TIRMAb-PILs is also demonstrated *in vivo*, as the confocal microscopy shows a down-regulation of the immunoreactive EGFR (Fig. 6, A–C). Other evidence for the suppression of the EGFR in the tumor *in vivo* is the 72–80% reduction in tumor vascular density in the tumors of mice treated with anti-EGFR gene therapy as compared with the vascular density of brain tumors in mice treated with saline (Table 4). The EGFR has a proangiogenic function in cancer (27). The results of the present study show that suppression of EGFR function in brain tumors results in a reduction in vascularization of the tumor (Table 4). The reduction in tumor vascular density is not a nonspecific effect of PIL administration, because there is no reduction in vascular density in control mouse brain (Table 4). A Blast analysis of nucleotide sequences of the human EGFR mRNA (accession no. X00588) and the mouse EGFR mRNA (accession no. AF275367) shows there is only 76% identity in the mouse sequence corresponding to 2529–2557 of the human EGFR. Therefore, the shRNA produced by clone 967 would not be expected to effect endogenous mouse EGFR expression.

The present studies show an 88% increase in survival time with weekly i.v. gene therapy using clone 967 encapsulated in

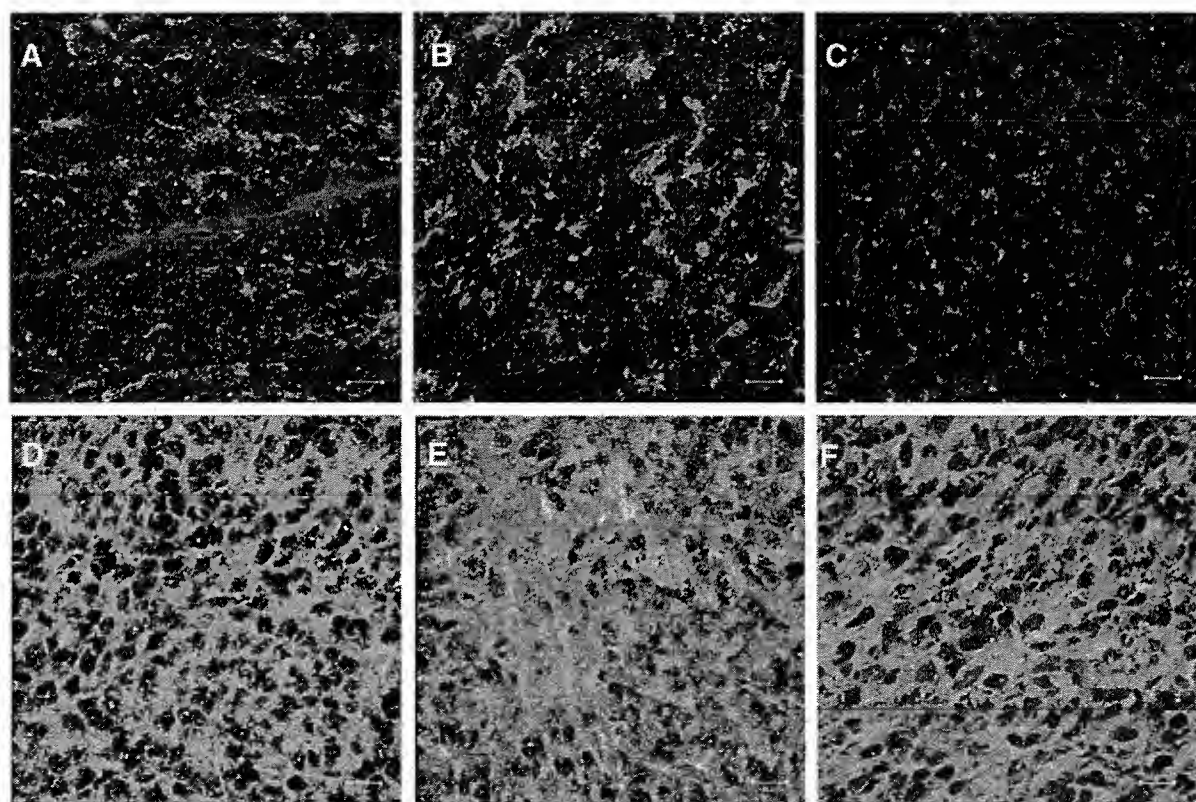


Fig. 6 Knock down of brain tumor epidermal growth factor receptor (EGFR) by RNA interference (RNAi). Confocal microscopy of intracranial glioma. Sections are shown for brain tumors from RNAi-treated mice (A–C) or saline-treated mice (D–F). The sections are doubly labeled with the murine 528 monoclonal antibody to the EGFR (green) and the rat 8D3 monoclonal antibody to the mouse transferrin receptor (red). There is decreased immunoreactive EGFR in the tumor cells in the RNAi-treated mice (A–C) relative to the saline treated mice (D–F). The saline treated animals died at 14–15 days after implantation (D–F), whereas the RNAi-treated animals died at 31 days (A), 33 days (B), and 34 days (C) after implantation, respectively, which was 5, 7, and 8 days after the last dose of i.v. RNAi gene therapy (Fig. 4).

HIRMAb/TfRMAb-PILs (Fig. 4). This increase in survival time is not a nonspecific effect of PIL administration, because prior work has shown no change in survival with the weekly administration of PILs carrying a luciferase expression plasmid (9). The increase in survival obtained with weekly i.v. anti-EGFR gene therapy is comparable with the prolongation of survival time in mice treated with high daily doses of the EGFR-tyrosine kinase inhibitor, ZD1839 (Iressa; Ref. 28). However, Iressa was not effective in the treatment of brain cancer expressing mutant forms of the EGFR (28). Many primary and metastatic brain cancers express mutations of the human EGFR (29, 30), and it is possible to design RNAi-based gene therapy that will knock down both wild-type and mutant EGFR mRNAs.

In summary, the present studies demonstrate that weekly i.v. RNAi gene therapy directed against the human EGFR causes an 88% increase in survival time in adult mice with intracranial human brain cancer. The high therapeutic efficacy of the PIL gene transfer technology is possible, because this approach delivers therapeutic genes to brain via the *trans*-vascular route (4). The PIL nonviral gene transfer technology could be used to simultaneously knock down tumorigenic genes and to replace mutated tumor suppressor genes in brain cancer. The efficacy of the PIL nonviral gene transfer technology has been demonstrated in primates, and levels of gene expression in primate brain are 50-fold greater than comparable levels of gene expression in rodent brain (31). PILs carrying therapeutic genes can be delivered to human brain cancer using genetically engineered MABs. A chimeric HIRMAb (32) has the same activity in terms of binding to the human BBB *in vitro*, or transport across the primate BBB *in vivo*, as the original murine HIRMAb used in these studies. Future clinical applications of the PIL approach to gene therapy of brain cancer should enable targeting of the therapeutic gene to the cancer cell with minimal general toxicity. Weekly administration of PILs has no toxic effects and causes no inflammation in brain (33). With regard to eliminating ectopic expression of the exogenous gene in noncancer cells, prior work has shown that region-specific gene expression is possible with tissue-specific gene promoters in either mice (34) or primates (35). It may be possible to restrict therapeutic gene expression to the cancer cell by putting the gene under the influence of a promoter taken from a gene selectively expressed in brain cancer. Alternatively, many solid cancers express mutant forms of the EGFR, which are produced from aberrantly processed mRNAs that contain nucleotide sequences not found in normal cells (36). These sequences can be used as shRNA targets to selectively knock down mutant transcripts in cancer cells.

REFERENCES

- Kuan CT, Wikstrand CJ, Bigner DD. EGF mutant receptor VIII as a molecular target in cancer therapy. *Endocr Relat Cancer* 2001;8:83–96.
- Nicholson RI, Gee JM, Harper ME. EGFR and cancer prognosis. *Eur J Cancer* 2001;37(Suppl 4):S9–15.
- Zhang RD, Price JE, Fujimaki T, Bucana CD, Fidler IJ. Differential permeability of the blood-brain barrier in experimental brain metastases produced by human neoplasms implanted into nude mice. *Am J Pathol* 1992;141:1115–24.
- Pardridge WM. Drug and gene delivery to the brain: the vascular route. *Neuron* 2002;36:555–8.
- Bendell JC, Domchek SM, Burstein HJ, et al. Central nervous system metastases in women who receive trastuzumab-based therapy for metastatic breast carcinoma. *Cancer* 2003;97:2972–7.
- Ram Z, Culver KW, Oshiro EM, et al. Therapy of malignant brain tumors by intratumoral implantation of retroviral vector-producing cells. *Nat Med* 1997;3:1354–61.
- Pardridge WM. Drug and gene targeting to the brain with molecular Trojan horses. *Nat Rev Drug Discov* 2002;1:131–9.
- Shi N, Pardridge WM. Non-invasive gene targeting to the brain. *Proc Natl Acad Sci USA* 2000;97:7567–72.
- Zhang Y, Zhu C, Pardridge WM. Antisense gene therapy of brain cancer with an artificial virus gene delivery system. *Mol Ther* 2002;6:67–72.
- Zhang Y, Lee HJ, Boado RJ, Pardridge WM. Receptor-mediated delivery of an antisense gene to human brain cancer cells. *J Gene Med* 2002;4:183–94.
- Makrides SC. Components of vectors for gene transfer and expression in mammalian cells. *Protein Expr Purif* 1999;17:183–202.
- Zhang Y, Boado RJ, Pardridge WM. Marked enhancement in gene expression by targeting the human insulin receptor. *J Gene Med* 2003;5:157–63.
- Snudden DK, Smith PR, Lai D, Ng MH, Griffin BE. Alterations in the structure of the EBV nuclear antigen, EBNA1, in epithelial cell tumours. *Oncogene* 1995;10:1545–52.
- McManus MT, Sharp PA. Gene silencing in mammals by small interfering RNAs. *Nat Rev Genet* 2002;3:737–47.
- Lee HJ, Engelhardt B, Lesley J, Bickel U, Pardridge WM. Targeting rat anti-mouse transferrin receptor monoclonal antibodies through the blood-brain barrier in the mouse. *J Pharmacol Exp Ther* 2000;292:1048–52.
- Pardridge WM, Kang Y-S, Buciak JL, Yang J. Human insulin receptor monoclonal antibody undergoes high affinity binding to human brain capillaries *in vitro* and rapid transcytosis through the blood-brain barrier *in vivo* in the primate. *Pharm Res* 1995;12:807–16.
- Paddison P, Caudy A, Bernstein E, Hannon G, Conklin D. Short hairpin RNAs (shRNAs) induce sequence-specific silencing in mammalian cells. *Genes Dev* 2002;16:948–58.
- Yu JY, Taylor J, DeRuiter SL, Vojtek AB, Turner DL. Simultaneous inhibition of GSK3 α and GSK3 β using hairpin siRNA expression vectors. *Mol Ther* 2003;7:228–36.
- Zhang Y, Boado RJ, Pardridge WM. *In vivo* knockdown of gene expression in brain cancer with intravenous RNAi in adult rats. *J Gene Med* 2003;5:1039–45.
- Pardridge WM. Gene targeting *in vivo* with pegylated immunoliposomes. *Methods Enzymol* 2003;373:507–28.
- Hernandez M, Barrero MJ, Crespo MS, Nieto ML. Lysophosphatidic acid inhibits Ca²⁺ signaling in response to epidermal growth factor receptor stimulation in human astrocytoma cells by a mechanism involving phospholipase C γ and a G α_i protein. *J Neurochem* 2000;75:1575–82.
- Stout CE, Costantin JL, Naus CC, Charles AC. Intercellular calcium signaling in astrocytes via ATP release through connexin hemichannels. *J Biol Chem* 2002;277:10482–8.
- Lal S, Lacroix M, Tofilon P, Fuller GN, Sawaya R, Lang FF. An implantable guide-screw system for brain tumor studies in small animals. *J Neurosurg* 2002;92:326–33.
- Kurihara A, Pardridge WM. Imaging brain tumors by targeting peptide radiopharmaceuticals through the blood-brain barrier. *Canc Res* 1999;54:6159–63.
- Nagy P, Arndt-Jovin DJ, Jovin TM. Small interfering RNAs suppress the expression of endogenous and GFP-fused epidermal growth factor receptor (erbB1) and induce apoptosis in erbB1-overexpressing cells. *Exp Cell Res* 2003;285:39–49.
- Ewald JA, Coker KJ, Price JO, Staros JV, Guyer CA. Stimulation of mitogenic pathways through kinase-impaired mutants of the epidermal growth factor receptor. *Exp Cell Res* 2001;268:262–73.

27. Abe T, Terada K, Wakimoto H, et al. PTEN decreases in vivo vascularization of experimental gliomas in spite of proangiogenic stimuli. *Cancer Res* 2003;63:2300–5.
28. Heimberger AB, Learn CA, Archer GE, et al. Brain tumors in mice are susceptible to blockade of epidermal growth factor receptor (EGFR) with the oral, specific, EGFR-tyrosine kinase inhibitor ZD1839 (iressa). *Clin Cancer Res* 2002;8:3496–502.
29. Luwor RB, Johns TG, Murone C, et al. Monoclonal antibody 806 inhibits the growth of tumor xenografts expressing either the de2–7 or amplified epidermal growth factor receptor (EGFR) but not wild-type EGFR. *Cancer Res* 2001;61:5355–61.
30. Lal A, Glazer CA, Martinson HM, et al. Mutant epidermal growth factor receptor up-regulates molecular effectors of tumor invasion. *Cancer Res* 2002;62:3335–9.
31. Zhang Y, Schlachetzki F, Pardridge WM. Global non-viral gene transfer to the primate brain following intravenous administration. *Mol Ther* 2003;7:11–8.
32. Coloma MJ, Lee HJ, Kurihara A, et al. Transport across the primate blood-brain barrier of a genetically engineered chimeric monoclonal antibody to the human insulin receptor. *Pharm Res* 2000;17:266–74.
33. Zhang Y-F, Boado RJ, Pardridge WM. Absence of toxicity of chronic weekly intravenous gene therapy with pegylated immunoliposomes. *Pharm Res* 2003;20:1779–85.
34. Shi N, Zhang Y, Boado RJ, Zhu C, Pardridge WM. Brain-specific expression of an exogenous gene after i.v. administration. *Proc Natl Acad Sci USA* 2001;98:12754–9.
35. Zhang Y, Schlachetzki F, Li JY, Boado RJ, Pardridge WM. Organ-specific gene expression in the Rhesus monkey eye following intravenous non-viral gene transfer. *Mol Vis* 2003;9:465–72.
36. Luo X, Gong X, Tang CK. Suppression of EGFRvIII-mediated proliferation and tumorigenesis of breast cancer cells by ribozyme. *Int J Cancer* 2003;104:716–21.